THE UNIVERSITY OF MICHIGAN

INDUSTRY PROGRAM OF THE COLLEGE OF ENGINEERING

THE AXISYMMETRIC RESPONSE OF A CLOSED SPHERICAL SHELL TO A NEARLY UNIFORM RADIAL IMPULSE

David A. Sonstegard

A dissertation submitted in partial fulfillment
of the requirements for the degree of
Doctor of Philosophy in the
University of Michigan
Department of Engineering Mechanics
1965

September, 1965

IP-716

Doctoral Committee:

Associate Professor Ivor K. McIvor, Chairman
Professor Emeritus Ruel V. Churchill
Professor Samuel K. Clark
Professor Donald T. Greenwood
Assistant Professor Roger D. Low

ACKNOWLEDGEMENTS

This area of research was suggested by Professor Ivor K. McIvor, my committee chairman. I gratefully acknowledge not only his invaluable instruction and guidance but also his personal enthusiasm and stimulus.

I express my sincere appreciation to all committee members for their interest, suggestions, and efforts.

I am indebted to the Alfred P. Sloan Foundation, the Consumers Power Company, the National Science Foundation, and the Ford Foundation for financial aid given to me during my graduate studies.

David Ansel Sonstegard

TABLE OF CONTENTS

LIST OF TABLES

LIST OF FIGURES

NOMENCLATURE

A_o, A_{nm}, A_{nc}	Constants of integration
A_n	Amplitude of critical deviation after complete energy transfer
E	Young's Modulus
E_b	Sum of maximum strains minus sum of midsurface strains
E_m	Sum of midsurface strains
L	Lagrangian
M_z	Momentum along polar axis
T	Kinetic energy
T_i	Energy imparted by impulsive pressure.
V	Potential energy
V_{max}	Maximum initial dimensionless velocity for $\sigma_y/E = 5(10)^{-3}$
V_N	Potential energy of Nth deviation after complete energy transfer
a	Radius of spherical shell
a_o, a_n	Coefficients of Legendre polynomial expansion of ζ.
b_n	Coefficients of associated Legendre polynomial expansion of ψ.
c	Wave velocity, $[E/\rho\ (1-\nu^2)]^{\frac{1}{2}}$
$ds_{o\xi}$, $ds_{o\eta}$	Midsurface elemental lengths before deformation
ds_ξ, ds_η	Midsurface elemental lengths after deformation
h	Shell thickness
$\vec{i}$, $\vec{j}$, $\vec{k}$	Unit vectors along x, y, z

$r, \Theta, \emptyset$	Spherical coordinates
t	Time
$\vec{t}_\xi, \vec{t}_\eta, \vec{n}$	Unit midsurface vectors
u	Meridional displacement
$\tilde{u}$	Meridional displacement with respect to moving reference
v_o	Uniform radial velocity
w	Radial displacement, a-r
$\tilde{w}$	Radial displacement with respect to moving reference
x, y, z	Cartesian coordinates
z	Distance from midsurface
$\Delta_o, \Delta_{nc}, \Delta_{nm}, \bar{\Delta}_{nc}, \bar{\Delta}_{nm}$	Amplitudes of motion due to arbitrary radial velocity distribution
T_f	Period of fundamental mode
Ω_n, μ_n	Parameters in Mathieu equation
α^2	Thickness parameter, $h^2/12a^2$
$\alpha_o, \alpha_{nc}, \alpha_{nm}$	Constants of integration
β	Angle between midsurface normal and radial ray
γ_o	Midsurface shear strain
δ_{nc}, δ_{nm}	Amplitude ratios
$\epsilon_{o\xi}, \epsilon_{o\eta}$	Midsurface normal strains
ϵ_n	Dimensionless perturbation quantity
$\epsilon_\xi, \epsilon_\eta$	Normal strains
ζ, ψ	Non-dimensional displacements

$\kappa_{o\xi}$, $\kappa_{o\eta}$	Midsurface curvatures
ν	Poisson's ratio, .3
ξ, η	Polar angles
ρ	Mass density
σ_o	Stress due to breathing mode
σ_y	Yield stress
σ_ξ, σ_η	Normal stresses
τ	Dimensionless time
$\overline{\tau}$	Dimensionless time, $\omega_o\tau$
ω_o, ω_{nc}, ω_{nm}	Angular frequencies of breathing, composite, and membrane modes respectively
ω_{2c}	Angular frequency of fundamental mode

CHAPTER 1

INTRODUCTION

Early studies of the dynamics of spherical shells were attempts to construct a theory of bells. Lord Rayleigh[1] considered an inextensional representation of the motion, i.e. he assumed that no stretching of the midsurface occurs during deformation. Love[2] took exception with the inextensional representation for two reasons: first, a closed shell can not undergo deformation without midsurface stretching; second, the restriction of inextensionality does not allow satisfaction of boundary conditions for a freely vibrating open shell, namely a bell.

Love's formulation of the problem[3] constitutes the classical bending theory of shells now known as Love's first approximation. This formulation includes both flexural and extensional effects. In actually solving the problem, however, Love assumed the vibrating shell to have negligible resistance to bending. He considered only extensional axisymmetric motion. Lamb[4] also used an extensional formulation in his study of the radial motion of closed spherical shells.

By the extensional approach Love found two sets of modes of vibration. Both sets contain an infinite number of modes. For the first set, called the upper set, the frequency spectrum is unbounded. All upper mode frequencies are higher than those of the second set, called the lower set, which has a bounded frequency spectrum. The boundedness of the lower set spectrum means that intervals between natural frequencies must become arbitrarily small, a physically untenable conclusion.

An analytical study by Silbiger[5] and experimental work by Baker[6] were based on the extensional analysis of Love. Naghdi and Kalnins[7] applied classical bending theory to obtain a solution for torsionless axisymmetric motion. Also included in this paper is a study of asymmetric motion based on extensional theory.

Kalnins[8], using classical bending theory, investigated the flexural vs membrane strain energy content of axisymmetric modes of vibration. Two mode sets were found. For one set the deformations were predominately extensional. For the other set, however, deformations were neither predominately extensional nor predominately inextensional. In the limiting case of infinitely large radius-to-thickness ratio this latter mode set was shown to degenerate to the lower set found by an extensional analysis. The paradoxical boundedness of the lower set frequency spectrum as predicted by an extensional analysis was thus shown to be caused by the effects of bending.

In 1883 Lord Rayleigh[9] reported an experiment in which a stretched string was attached to one prong of a tuning fork. The fork vibrated in the direction of the string. Lateral vibrations of the string of frequency f were produced by fork vibrations of frequency 2f. This phenomenon is termed heteroparametric excitation (the prefix "hetero" being commonly omitted). Parametric effects occur frequently in mechanics. Numerous examples are presented by Minorsky[10]. Bolotin's book on dynamic stability[11] is devoted entirely to heteroparametric excitation.

Autoparametric excitation is a similar phenomenon. An example of this behavior is a mass suspended on a spring as reported by Gorelik and Witt (see[10], p. 506). The system is allowed two degrees of freedom, spring elongation and plane pendulum motion. For certain elongation mode-pendulum mode frequency relations nonlinear coupling between the modes alters the initially excited motion markedly. Energy originally imparted to elongation motion is transferred to pendulum motion.

Both hetero-and auto-parametric excitation are generally governed by differential equations with periodic coefficients. Two distinctly different physical phenomena occur however. For heteroparametric excitation an external energy source, such as Lord Rayleigh's tuning fork, produces the parametric effect. For autoparametric behavior no outside energy is supplied to the initially excited system, only an energy redistribution occurs. The energy exchange is due to nonlinear coupling between distinct modes of motion.

Autoparametric behavior has been reported for the cylindrical shell by Goodier and McIvor[12]. Here the energy exchange is effected by nonlinear coupling between extensional and inextensional mode sets. Analogously, two mode sets exist for the closed spherical shell. However, one mode set is not of a distinct extensional or inextensional character. The possibility of autoparametric excitation is, therefore, of particular interest and gave impetus to this investigation.

CHAPTER 2

A NONLINEAR FORMULATION

In this chapter a Lagrangian representation of spherical shell deformation is presented. The formulation is restricted to torsionless axisymmetric motion. Nonlinear equations of motion are derived for a second order theory which is restricted to small deformation of thin shells.

2.1 Representation of Deformation

The undeformed configuration is the closed spherical shell of radius a. A point P on the undeformed midsurface is located by angles ξ and η, Figure 1a. During deformation P goes to P* on the deformed midsurface and is located by spherical coordinates r, Θ, and ϕ, Figure 1b.

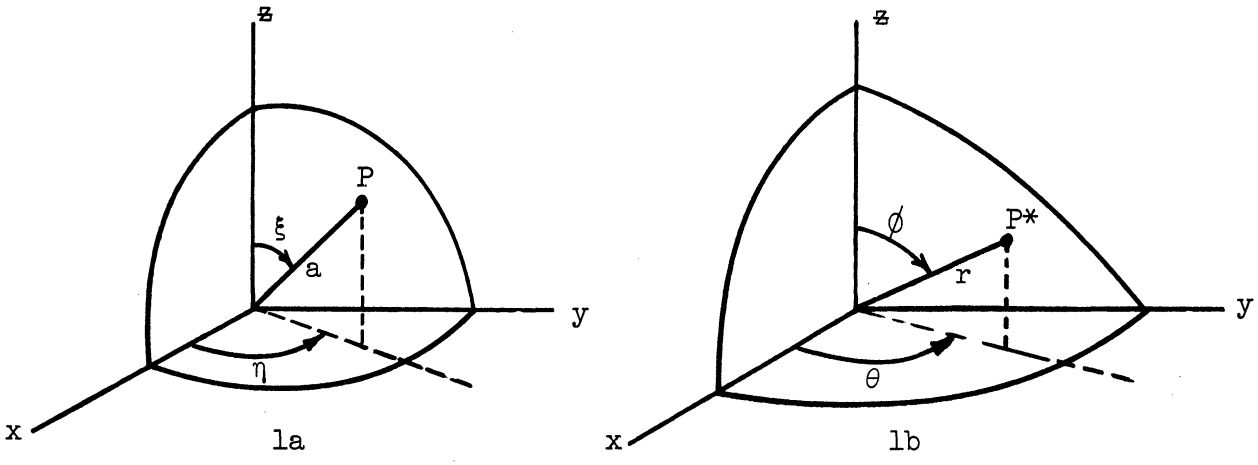

Figure 1. Undeformed and Deformed Configurations

Motion of point P is described in the Lagrangian sense. The deformed state coordinates are taken as functions of initial position and time, i.e.

$$r = r(\xi, \eta, t) \tag{2.1.1a}$$

$$\Theta = \Theta(\xi, \eta, t) \tag{2.1.1b}$$

$$\phi = \phi(\xi, \eta, t) \tag{2.1.1c}$$

2.2 Midsurface Quantities

In the Lagrangian representation of Section 2.1 unit vectors on the midsurface are expressed as

$$\vec{t}_\xi = \frac{1}{[\dot{r}^2 + r^2\dot{\Theta}^2\sin^2\phi + r^2\dot{\phi}^2]^{\frac{1}{2}}} \Big\{ [\dot{r}\sin\phi\cos\Theta - r\dot{\Theta}\sin\phi\sin\Theta + r\dot{\phi}\cos\phi\cos\Theta]\,\vec{i} + [\dot{r}\sin\phi\sin\Theta + r\dot{\Theta}\sin\phi\cos\Theta + r\dot{\phi}\cos\phi\sin\Theta]\,\vec{j} + [\dot{r}\cos\phi - r\dot{\phi}\sin\phi]\,\vec{k} \Big\} \tag{2.2.1a}$$

$$\vec{t}_\eta = \frac{1}{[r'^2 + r^2\Theta'^2\sin^2\phi + r^2\phi'^2]^{\frac{1}{2}}} \Big\{ r'\sin\phi\cos\Theta - r\Theta'\sin\phi\sin\Theta + r\phi'\cos\phi\cos\Theta]\,\vec{i} + [r'\sin\phi\sin\Theta + r\Theta'\sin\phi\cos\Theta + r\phi'\cos\phi\sin\Theta]\,\vec{j} + [r'\cos\phi - r\phi'\sin\phi]\,\vec{k} \Big\} \tag{2.2.1b}$$

where $\vec{i}$, $\vec{j}$, $\vec{k}$ are unit vectors along x, y, z respectively, the dot denotes $\partial/\partial\xi$ and the prime denotes $\partial/\partial\eta$.

From differential geometry the normal strain $\epsilon_{o\xi}$ and the curvature $\kappa_{o\xi}$ of the midsurface along $\vec{t}_\xi$ are

$$\epsilon_{o\xi} = \frac{1}{a}\,[\dot{r}^2 + r^2\dot{\Theta}^2\sin^2\phi + r^2\dot{\phi}^2]^{\frac{1}{2}} - 1 \tag{2.2.2a}$$

$$\kappa_{o\xi} = \frac{1}{[\dot{r}^2 + r^2\dot{\Theta}^2\mathrm{Sin}^2\phi + r^2\dot{\phi}^2]^{3/2}} \Big\{ 4\dot{r}^4\dot{\Theta}^2\mathrm{Sin}^2\phi + 4\dot{r}^4\dot{\phi}^2$$

$$+ r\,[-4\dot{r}^2\ddot{r}\,(\dot{\Theta}^2\mathrm{Sin}^2\phi + \dot{\phi}^2) + 4\dot{r}^3\,(\dot{\Theta}\,\ddot{\Theta}\mathrm{Sin}^2\phi + \dot{\Theta}^2\dot{\phi}\,\mathrm{Sin}\phi\mathrm{Cos}\phi + \dot{\phi}\,\ddot{\phi}]$$

$$+ r^2[\dot{r}^2(\ddot{\Theta}^2\mathrm{Sin}^2\phi + \dot{\Theta}^4\mathrm{Sin}^2\phi + 3\dot{\Theta}^4\mathrm{Sin}^4\phi + \ddot{\phi}^2 + 4\dot{\Theta}^2\dot{\phi}^2$$

$$+ 4\dot{\Theta}^2\dot{\phi}^2\mathrm{Sin}^2\phi + 4\,\dot{\Theta}\,\ddot{\Theta}\,\dot{\phi}\mathrm{Sin}\phi\mathrm{Cos}\phi - 2\dot{\Theta}^2\ddot{\phi}\mathrm{Sin}\phi\mathrm{Cos}\phi + 4\dot{\phi}^4\,)$$

$$- 2\,\dot{r}\,\ddot{r}(\dot{\Theta}\,\ddot{\Theta}\mathrm{Sin}^2\phi + \dot{\Theta}^2\dot{\phi}\mathrm{Sin}\phi\mathrm{Cos}\phi + \dot{\phi}\,\ddot{\phi}) + \ddot{r}^2(\dot{\Theta}^2\mathrm{Sin}^2\phi + \dot{\phi}^2)]$$

$$+ r^3[2\dot{r}\,(\dot{\Theta}^3\ddot{\Theta}\mathrm{Sin}^4\phi + \dot{\Theta}^4\dot{\phi}\mathrm{Sin}^3\phi\mathrm{Cos}\phi + \dot{\Theta}^2\dot{\phi}\,\ddot{\phi}\mathrm{Sin}^2\phi$$

$$+ \dot{\Theta}\,\ddot{\Theta}\,\dot{\phi}^2\mathrm{Sin}^2\phi + \dot{\Theta}^2\dot{\phi}^3\mathrm{Sin}\phi\mathrm{Cos}\phi + \dot{\phi}^3\ddot{\phi}\,)$$

$$- 2\,\ddot{r}(\dot{\Theta}^4\mathrm{Sin}^4\phi + 2\dot{\Theta}^2\dot{\phi}^2\mathrm{Sin}^2\phi + \dot{\phi}^4)]$$

$$+ r^4[\dot{\Theta}^6\mathrm{Sin}^4\phi + \dot{\Theta}^4(3\dot{\phi}^2\mathrm{Sin}^2\phi + \dot{\phi}^2\mathrm{Sin}^2\phi\mathrm{Cos}^2\phi - 2\ddot{\phi}\mathrm{Sin}^3\phi\mathrm{Cos}\phi)$$

$$+ 2\dot{\Theta}^3\ddot{\Theta}\,\dot{\phi}\mathrm{Sin}^3\phi\mathrm{Cos}\phi + \dot{\Theta}^2(\ddot{\phi}^2\mathrm{Sin}^2\phi + 3\,\dot{\phi}^4 + \dot{\phi}^4\mathrm{Cos}^2\phi$$

$$- 4\,\dot{\phi}^2\ddot{\phi}\mathrm{Sin}\phi\mathrm{Cos}\phi) + \ddot{\Theta}^2\dot{\phi}^2\mathrm{Sin}^2\phi$$

$$+ 2\,\dot{\Theta}\,\ddot{\Theta}\,\dot{\phi}(2\,\dot{\phi}^2\mathrm{Sin}\phi\mathrm{Cos}\phi - \ddot{\phi}\mathrm{Sin}^2\phi) + \dot{\phi}^6]\Big\}^{\frac{1}{2}} \qquad (2.2.2b)$$

Similarly, along $\vec{t}_\eta$ the normal strain and curvature are

$$\epsilon_{o\eta} = \frac{1}{a\ \mathrm{Sin}\ \xi}\,[r'^2 + r^2\Theta'^2\mathrm{Sin}^2\phi + r^2\phi'^2] - 1 \qquad (2.2.2c)$$

$$\kappa_{o\eta} \sim \kappa_{o\xi} \text{ with dots replaced by primes} \qquad (2.2.2d)$$

The midsurface shear strain γ_o is

$$\gamma_o = \frac{\dot{r}\, r' + r^2\dot{\Theta}\,\Theta'\mathrm{Sin}^2\phi + r^2\dot{\phi}\,\phi'}{[\dot{r}^2 + r^2\dot{\Theta}^2\mathrm{Sin}^2\phi + r^2\dot{\phi}^2]^{\frac{1}{2}}\,[r'^2 + r^2\Theta'^2\mathrm{Sin}^2\phi + r^2\phi'^2]^{\frac{1}{2}}} \qquad (2.2.2e)$$

One of the difficulties encountered in even a small displacement approximation of (2.2.2) is the non-orthogonality of the ξ-η curvilinear coordinate system. Orthogonality results from the introduction of axisymmetry, whereby

$$r' = \phi' = 0 \qquad (2.2.3a)$$

$$\Theta - \eta = 0 \qquad (2.2.3b)$$

The latter requirement precludes circumferential or torsional displacements.

Imposing conditions (2.2.3) on (2.2.2) yields the following midsurface strain and curvature expressions:

$$\epsilon_{o\xi} = \frac{1}{a}\,[\dot{r}^2 + r^2\dot{\phi}^2]^{\frac{1}{2}} - 1 \qquad (2.2.4a)$$

$$\epsilon_{o\eta} = \frac{r\ \mathrm{Sin}\ \phi}{a\ \mathrm{Sin}\ \xi} - 1 \qquad (2.2.4b)$$

$$\kappa_{o\xi} = \frac{1}{[\dot{r}^2 + r^2\dot{\phi}^2]^{3/2}} \Big\{ 4\dot{r}^4\dot{\phi}^2 + r\,[4\dot{r}^3\dot{\phi}\,\ddot{\phi} - 4\dot{r}^2\ddot{r}\,\dot{\phi}^2]$$

$$+ r^2[\dot{r}^2(\ddot{\phi}^2 + 4\dot{\phi}^4) - 2\,\dot{r}\,\ddot{r}\,\dot{\phi}\,\ddot{\phi} + \ddot{r}^2\dot{\phi}^2]$$

$$+ r^3[2\dot{r}\,\dot{\phi}^3\ddot{\phi} - 2\,\ddot{r}\,\dot{\phi}^4] + r^4\dot{\phi}^6 \Big\}^{\frac{1}{2}} \qquad (2.2.4c)$$

$$\kappa_{o\eta} = \frac{1}{a\ \mathrm{Sin}\ \phi} \qquad (2.2.4d)$$

$$\gamma_o = 0 \qquad (2.2.4e)$$

2.3 Strain-Midsurface Quantities-Stress Relations

An element as viewed on a meridional cut before and after deformation is shown in Figure 2.

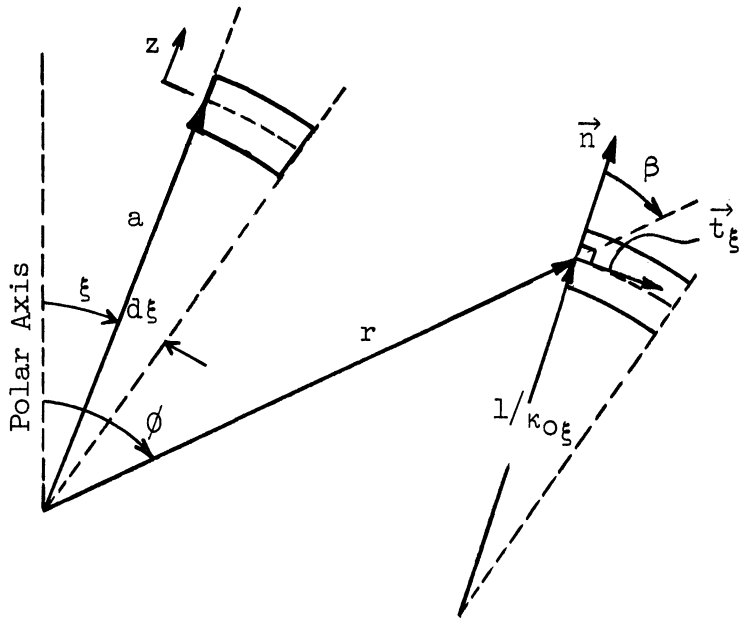

Figure 2. View on a Meridional Cut

The angle between the surface normal vector $\vec{n}$ and the radial ray may be expressed as

$$\beta = \tan^{-1} \frac{\dot{r}}{r\,\dot{\phi}} \tag{2.3.1}$$

Normals to the undeformed midsurface are assumed to be unstretched and to remain normal to the midsurface after deformation.

Midsurface elemental lengths along $\vec{t}_\xi$ before and after deformation are respectively

$$ds_{o\xi} = a\,d\xi \tag{2.3.2a}$$

$$ds_\xi = (1 + \epsilon_{o\xi})\, a\,d\xi \tag{2.3.2b}$$

The normal strain along $\vec{t}_\xi$ a distance z from the midsurface follows as

$$\epsilon_\xi = \frac{(1 + \epsilon_{o\xi})\,(1 + z\,\kappa_{o\xi}) - (1 + {}^{z}/a)}{1 + {}^{z}/a} \qquad (2.3.3)$$

The right side of equation (2.3.3) is expanded in powers of z/a. The shell is assumed sufficiently thin to allow neglect of z^2/a^2 with respect to unity. The expansion then yields

$$\epsilon_\xi = \epsilon_{o\xi} + z(\kappa_{o\xi} - \frac{1}{a})\,(1 + \epsilon_{o\xi})\,(1 - \frac{z}{a}) \qquad (2.3.4)$$

A deformed element as again viewed on a meridional cut is shown in Figure 3.

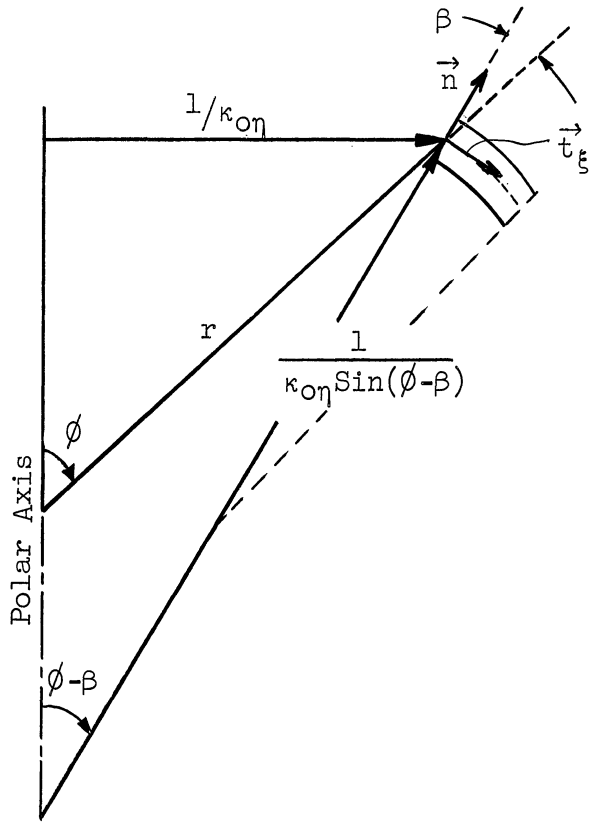

Figure 3. View on a Meridional Cut

Midsurface element lengths along $\vec{t}_\eta$ before and after deformation are respectively

$$ds_{o\eta} = a \text{ Sin } \xi \, d\eta \tag{2.3.5a}$$

$$ds_\eta = (1 + \epsilon_{o\eta}) \, a \text{ Sin } \xi \, d\eta \tag{2.3.5b}$$

The midsurface strain along $\vec{t}_\eta$ a distance z from the midsurface is

$$\epsilon_\eta = \frac{[1 + z \, \kappa_{o\eta} \text{ Sin } (\phi - \beta)] \, [1 + \epsilon_{o\eta}] - (1 + {}^{z}/_{a})}{1 + {}^{z}/_{a}} \tag{2.3.6}$$

Again neglecting z^2/a^2 with respect to unity, expansion of the right side of (2.3.6) in powers of z/a gives

$$\epsilon_\eta = \epsilon_{o\eta} + z \left[\kappa_{o\eta} \text{ Sin } (\phi - \beta) - \frac{1}{a}\right] (1 + \epsilon_{o\eta}) \, (1 - z/a) \tag{2.3.7}$$

The continuum is assumed to be isotropic and homogeneous. Neglecting stress normal to the midsurface, Hooke's Law yields biaxial stress-strain relations. They are

$$\sigma_\xi = \frac{E}{1 - \nu^2} (\epsilon_\xi + \nu \, \epsilon_\eta) \tag{2.3.8a}$$

$$\sigma_\eta = \frac{E}{1 - \nu^2} (\epsilon_\eta + \nu \, \epsilon_\xi) \tag{2.3.8b}$$

where E is Young's Modulus and ν is Poisson's Ratio.

2.4 Equations of Motion for Small Displacements

Equations of motion may be derived by an energy formulation or by consideration of the equilibrium of a shell element. Since the energy formulation is convenient in the subsequent analysis it is to be used here.

Assuming negligible rotary inertia the kinetic energy T is

$$T = \frac{1}{2}\int_{\text{volume}} \rho \left[\left(\frac{\partial r}{\partial t}\right)^2 + r^2 \left(\frac{\partial \phi}{\partial t}\right)^2 \right] dV \qquad (2.4.1)$$

where ρ is the mass density.

A non-dimensional time τ, a non-dimensional radial displacement ζ, and an angular meridional displacement ψ are defined as

$$\tau = \frac{1}{a}\left[\frac{E}{\rho\,(1-\nu^2)}\right]^{\frac{1}{2}} t \qquad (2.4.2a)$$

$$\zeta = \frac{1}{a}(a - r) \qquad (2.4.2b)$$

$$\psi = \phi - \xi \qquad (2.4.2c)$$

Substitution of τ, ζ, and ψ into (2.4.1) followed by an integration over the circumference and thickness yields

$$T = \frac{\Pi a^2 E h}{1-\nu^2}\int_0^{\Pi} \left[\left(\frac{\partial \zeta}{\partial \tau}\right)^2 + (1-2\zeta)\left(\frac{\partial \psi}{\partial \tau}\right)^2\right] \text{Sin } \xi \; d\,\xi \qquad (2.4.3)$$

Displacements and their derivatives are assumed small; therefore, terms of order greater than three are neglected in (2.4.3).

For free vibrations of the assumed conservative system the potential energy V is the strain energy stored during deformation, namely

$$V = \frac{1}{2}\int_{\text{volume}} \left(\sigma_\xi \epsilon_\xi + \sigma_\eta \epsilon_\eta\right) dV \qquad (2.4.4)$$

From substitution of stress-strain relations (2.3.8) there results

$$V = \frac{E}{2(1-\nu^2)}\int_{\text{volume}} [\epsilon_\xi^2 + 2\,\nu\,\epsilon_\xi \epsilon_\eta + \epsilon_\eta^2]\, dV \qquad (2.4.5)$$

The midsurface quantities and the angle β may be expressed in terms of ζ and ψ by substitution of (2.4.2) into (2.2.4) and (2.3.1). The results are

$$\epsilon_{o\xi} = \dot{\psi} - \zeta - \zeta\,\dot{\psi} + \frac{1}{2}\,\dot{\zeta}^2 \tag{2.4.6a}$$

$$\epsilon_{o\eta} = -\zeta + \psi\,\mathrm{Cot}\,\xi - \frac{1}{2}\,\psi^2 - \zeta\,\psi\,\mathrm{Cot}\,\xi \tag{2.4.6b}$$

$$\kappa_{o\xi} = \frac{1}{a}\left(1 + \zeta + \ddot{\zeta} + \zeta^2 + \frac{1}{2}\,\dot{\zeta}^2 + 2\,\zeta\,\ddot{\zeta} - \dot{\zeta}\,\ddot{\psi} - 2\,\ddot{\zeta}\,\dot{\psi}\right) \tag{2.4.6c}$$

$$\kappa_{o\eta} = \frac{1}{a\,\mathrm{Sin}\,\xi}\left(1 + \zeta - \psi\,\mathrm{Cot}\,\xi + \zeta^2 + \psi^2\,\mathrm{Csc}^2\,\xi - \psi\,\zeta\,\mathrm{Cot}\,\xi\right) \tag{2.4.6d}$$

$$\beta = -\dot{\zeta} + \dot{\zeta}\,\dot{\psi} - \zeta\,\dot{\zeta} \tag{2.4.6e}$$

Consistent with the retention of third order terms in (2.4.3), terms of order greater than two are neglected in (2.4.6).

The strain energy (2.4.5) may now be expressed in terms of the midsurface quantities by substitution of (2.3.6) and (2.3.7), and subsequently in terms of ζ and ψ by substitution of (2.4.6). Terms up to the third order are again retained after integration over the circumference and thickness. These terms occur in two forms, the first with coefficient h and the second with coefficient $h^3/12a^2$. To be consistent with the thin shell assumption of Section 2.3, third order terms of the latter form are neglected. The resulting potential energy expression is

$$V = \frac{\Pi\, a^2 E\, h}{1 - \nu^2} \int_0^{\Pi} \Big\langle \dot{\psi}^2 + \psi^2 \mathrm{Cot}^2\xi + 2(1+\nu)\,(\zeta^2$$

$$- \zeta\,\psi\,\mathrm{Cot}\,\xi - \zeta\,\psi + \zeta^2\psi\,\mathrm{Cot}\,\xi + \zeta^2\dot{\psi}) - 2\,\zeta\,\dot{\psi}^2$$

$$+ \dot{\zeta}^2\dot{\psi} - \zeta\,\dot{\zeta}^2 + \zeta\,\psi^2 - \psi^3\mathrm{Cot}\,\xi - 2\,\zeta\,\psi^2\mathrm{Cot}^2\xi$$

$$+ 2\nu(\psi\,\dot{\psi}\,\mathrm{Cot}\,\xi - \tfrac{1}{2}\psi^2\dot{\psi} - 2\,\zeta\,\psi\,\dot{\psi}\,\mathrm{Cot}\,\xi + \tfrac{1}{2}\,\zeta\,\psi^2$$

$$- \tfrac{1}{2}\,\zeta\,\dot{\zeta}^2 + \tfrac{1}{2}\,\dot{\zeta}^2\psi\,\mathrm{Cot}\,\xi) + \alpha^2[\dot{\psi}^2 + \psi^2\mathrm{Cot}^2\xi$$

$$+ 2\,\ddot{\zeta}\,\dot{\psi} + 2\,\dot{\zeta}\,\psi\,\mathrm{Cot}^2\xi + \ddot{\zeta}^2 + \dot{\zeta}^2\,\mathrm{Cot}^2\xi$$

$$+ 2\nu(\psi\,\dot{\psi}\,\mathrm{Cot}\,\xi + \dot{\zeta}\,\dot{\psi}\,\mathrm{Cot}\,\xi + \ddot{\zeta}\,\psi\,\mathrm{Cot}\,\xi$$

$$+ \dot{\zeta}\,\ddot{\zeta}\,\mathrm{Cot}\,\xi)]\Big\rangle\,\mathrm{Sin}\,\xi\,d\,\xi \qquad (2.4.7)$$

where α^2 , a thickness parameter, is defined as

$$\alpha^2 = \frac{h^2}{12a^2}$$

The Lagrangian L is defined as the difference between the kinetic and potential energies, i.e.

$$L = T - V \qquad (2.4.8)$$

Hamilton's Principle states that the motion realized in nature is that particular one for which the time integral of L assumes a stationary value. The principle may be expressed

$$\delta \int_{t_1}^{t_2} L\,dt = 0 \qquad (2.4.9)$$

where t_1 and t_2 are arbitrary but fixed times, and δ denotes the customary variational operation.

The Lagrangian is expressed as (2.4.3) minus (2.4.7). In order to satisfy (2.4.9), ζ and ψ must satisfy the two nonlinear partial differential equations (see, for example, Hildebrand[13], p. 137)

$$\ddot{\psi} + \dot{\psi}\,\mathrm{Cot}\,\xi - \psi(\nu + \mathrm{Cot}^2\xi) - \dot{\zeta}(1 + \nu) - 2\,\dot{\zeta}\,\dot{\psi}$$

$$- 2\,\zeta\,\ddot{\psi} + \zeta\,\ddot{\zeta} - 2\,\zeta\,\dot{\psi}\,\mathrm{Cot}\,\xi + \tfrac{1}{2}\,\dot{\zeta}^2\mathrm{Cot}\,\xi\,(1 - \nu)$$

$$+ \tfrac{1}{2}\,\psi^2\mathrm{Cot}\,\xi(3 - \nu) - \zeta\,\psi(1 - \nu - 2\,\mathrm{Cot}^2\xi) - 2\,\nu\,\dot{\zeta}\,\psi\,\mathrm{Cot}\,\xi$$

$$+ 2\,\zeta\,\dot{\zeta}\,(1 + \nu) + \alpha^2[\ddot{\psi} + \dot{\psi}\,\mathrm{Cot}\,\xi - \psi(\nu + \mathrm{Cot}^2\xi)$$

$$+ \dddot{\zeta} + \ddot{\zeta}\,\mathrm{Cot}\,\xi - \dot{\zeta}(\nu + \mathrm{Cot}^2\xi)]$$

$$= (1 - 2\,\zeta)\,\frac{\partial^2\psi}{\partial\tau^2} - 2\,\frac{\partial\zeta}{\partial\tau}\cdot\frac{\partial\psi}{\partial\tau} \qquad (2.4.10a)$$

$$(1 + \nu)\,(\dot{\psi} + \psi\,\mathrm{Cot}\,\xi - 2\,\zeta - \zeta\,\dot{\psi} - \tfrac{1}{2}\,\dot{\zeta}^2 - \tfrac{1}{2}\,\psi^2 - 2\,\zeta\,\psi\,\mathrm{Cot}\,\xi$$

$$- \zeta\,\ddot{\zeta} - \zeta\,\dot{\zeta}\,\mathrm{Cot}\,\xi + \dot{\zeta}\,\dot{\psi}) + \dot{\psi}^2 + \ddot{\zeta}\,\dot{\psi} + \psi^2\mathrm{Cot}\,\xi$$

$$+ \nu(2\,\psi\,\dot{\psi}\,\mathrm{Cot}\,\xi + \ddot{\zeta}\,\psi\,\mathrm{Cot}\,\xi - \dot{\zeta}\,\psi)$$

$$- \alpha^2[\dddot{\psi} + 2\ddot{\psi}\mathrm{Cot}\,\xi - \dot{\psi}(1 + \nu + \mathrm{Cot}^2\xi) + \psi\,\mathrm{Cot}\,\xi(2 - \nu + \mathrm{Cot}^2\xi)$$

$$+ \ddddot{\zeta} + 2\dddot{\zeta}\mathrm{Cot}\,\xi - \ddot{\zeta}(1 + \nu + \mathrm{Cot}^2\xi) + \dot{\zeta}\,\mathrm{Cot}\,\xi(2 - \nu + \mathrm{Cot}^2\xi)]$$

$$= \frac{\partial^2\zeta}{\partial\tau^2} + \left(\frac{\partial\psi}{\partial\tau}\right)^2 \qquad (2.4.10b)$$

Satisfaction of (2.4.9) also imposes natural boundary conditions on ζ and ψ. These conditions are, at $\xi = 0$ and Π,

$$\delta\zeta\Big\langle [\dot{\xi}\,\dot{\psi} - \zeta\,\dot{\xi} + \nu(\dot{\xi}\,\psi\,\mathrm{Cot}\,\xi - \zeta\,\dot{\xi})]\ \mathrm{Sin}\,\xi$$

$$+ \alpha^2[(\psi + \dot{\xi})\,(1 - \nu)\,\mathrm{Cos}^2\xi\,\mathrm{Csc}\,\xi - (\ddot{\psi} + \dddot{\xi})\ \mathrm{Sin}\,\xi$$

$$+ \nu(\psi + \dot{\xi})\,\mathrm{Csc}\,\xi - (\dot{\psi} - \ddot{\xi})\,\mathrm{Cos}\,\xi]\Big\rangle = 0 \qquad (2.4.11a)$$

$$\delta\dot{\zeta}\Big\langle [\dot{\psi} + \ddot{\xi} + \nu(\psi + \dot{\xi})\,\mathrm{Cot}\,\xi]\ \mathrm{Sin}\,\xi\Big\rangle = 0 \qquad (2.4.11b)$$

$$\delta\psi\Big\langle \{\dot{\psi} - \zeta + \zeta^2 - 2\,\zeta\,\dot{\psi} + \dot{\xi}^2 + \nu(-\zeta + \zeta^2 + \psi\,\mathrm{Cot}\,\zeta - \tfrac{1}{2}\psi^2$$

$$- 2\,\zeta\,\psi\,\mathrm{Cot}\,\xi) + \alpha^2[\dot{\psi} + \ddot{\xi} + \nu(\psi\,\mathrm{Cot}\,\xi$$

$$+ \dot{\xi}\,\mathrm{Cot}\,\xi]\}\ \ \mathrm{Sin}\,\xi\Big\rangle = 0 \qquad (2.4.11c)$$

CHAPTER 3

A LINEAR STUDY

The linear motion of a closed spherical shell has received the attention of numerous investigators. A brief survey is contained in Chapter 1. Available results, however, are not in a form convenient for the present nonlinear study. A linear analysis is therefore presented in this chapter.

3.1 The Linear Solution

For sufficiently small deformations the second order terms in (2.4.10) may be neglected. The resulting expressions constitute the classical bending formulation of torsionless axisymmetric motion. The two linear partial differential equations governing free motions are

$$\ddot{\psi} + \dot{\psi}\,\mathrm{Cot}\,\xi - \psi(\nu + \mathrm{Cot}^2\,\xi) - \dot{\zeta}(1+\nu)$$

$$+ \alpha^2[\ddot{\psi} + \dot{\psi}\,\mathrm{Cot}\,\xi - \psi(\nu + \mathrm{Cot}^2\xi) + \dddot{\zeta} + \ddot{\zeta}\,\mathrm{Cot}\,\xi$$

$$- \dot{\zeta}\,(\nu + \mathrm{Cot}^2\,\zeta)] \;=\; \frac{\partial^2\psi}{\partial\tau^2} \qquad (3.1.1a)$$

$$(1+\nu)\,(\dot{\psi} + \psi\,\mathrm{Cot}\,\xi - 2\,\zeta) - \alpha^2\,[\dddot{\psi} + 2\,\ddot{\psi}\,\mathrm{Cot}\,\xi$$

$$- \dot{\psi}(1+\nu+\mathrm{Cot}^2\xi) + \psi\,\mathrm{Cot}\,\xi(2 - \nu + \mathrm{Cot}^2\xi)$$

$$+ \ddddot{\zeta} + 2\,\dddot{\zeta}\,\mathrm{Cot}\,\xi - \ddot{\zeta}(1 + \nu + \mathrm{Cot}^2\xi) + \dot{\zeta}\,\mathrm{Cot}\,\xi(2 - \nu$$

$$+ \mathrm{Cot}^2\xi)] \;=\; \frac{\partial^2\zeta}{\partial\tau^2} \qquad (3.1.1b)$$

The displacement ζ is expanded in a series of Legendre polynomials of the first kind. Legendre polynomials of the second kind are singular at the poles and are therefore omitted from the expansion. The expansion is

$$\zeta = \sum_{n=0}^{\infty} a_n (\tau) P_n (\text{Cos } \xi) \qquad (3.1.2)$$

The displacement ψ is expanded in a series of associated Legendre polynomials of the first order, first kind. Again those of the second kind are omitted. Then[1]

$$\psi = \sum_{n=1}^{\infty} b_n (\tau) \dot{P}_n (\text{Cos } \xi) \qquad (3.1.3)$$

The assumed forms (3.1.2) and (3.1.3) satisfy the natural boundary conditions (2.4.11).

Substitution of (3.1.2) and (3.1.3) into (3.1.1) and repeated use of the Legendre relation

$$\ddot{P}_n(\text{Cos } \xi) + \dot{P}_n(\text{Cos } \xi) \text{ Cot } \xi + n(n + 1) P_n(\text{Cos } \xi) = 0 \qquad (3.1.4)$$

yield

$$\frac{D^2 a_o}{D\tau^2} + 2(1 + \nu) a_o = 0 \qquad (3.1.5a)$$

---

1 $\dot{P}_n(\text{Cos } \xi)$ is more commonly expressed with the change of variable

$$x = \text{Cos } \xi$$

whereby

$$\dot{P}_n(\text{Cos } \xi) = - (1 - x^2)^{\frac{1}{2}} \frac{d}{dx} [P_n(x)] = P_n^1(x)$$

See, for example, Magnus and Oberhettinger[14], p. 53.

$$b_n[1 - \nu - n(n+1)]\,(1+\alpha^2) - a_n\{1 + \nu - \alpha^2[1 - \nu - n(n+1)]\}$$

$$= \frac{D^2 b_n}{D\tau^2} \qquad n \geq 1 \tag{3.1.5b}$$

$$- b_n(1+\nu)n(n+1) - 2\,a_n\,(1+\nu)$$

$$- \alpha^2(a_n + b_n)\,[n^2(n+1)^2 - (1-\nu)\,n(n+1)]$$

$$= \frac{D^2 a_n}{D\tau^2} \qquad n \geq 1 \tag{3.1.5c}$$

The solution of (3.1.5) is

$$a_o = A_o \operatorname{Sin}(\omega_o \tau + \alpha_o) \tag{3.1.6a}$$

$$a_n = A_{nm} \operatorname{Sin}(\omega_{nm}\tau + \alpha_{nm})$$

$$+ A_{nc} \operatorname{Sin}(\omega_{nc}\tau + \alpha_{nc}) \quad n \geq 1 \tag{3.1.6b}$$

$$b_n = \delta_{nm} A_{nm} \operatorname{Sin}(\omega_{nm}\tau + \alpha_{nm})$$

$$+ \delta_{nc} A_{nc} \operatorname{Sin}(\omega_{nc}\tau + \alpha_{nc}) \quad n \geq 1 \tag{3.1.6c}$$

where A_o, A_{nm}, A_{nc}, α_o, α_{nm}, and α_{nc} are arbitrary constants.

The amplitude ratios are

$$\delta_{nm} = \frac{1 + \nu - \alpha^2(1-\nu) + \alpha^2\, n(n+1)}{[1 - \nu - n(n+1)]\,(1+\alpha^2) + \omega_{nm}^2} \tag{3.1.7a}$$

$$\delta_{nc} = \frac{1 + \nu - \alpha^2 (1 - \nu) + \alpha^2 n(n + 1)}{[1 - \nu - n(n + 1)] (1+\alpha^2) + \omega_{nc}^2} \tag{3.1.7b}$$

Angular frequency ω_o is

$$\omega_o = [2(1 + \nu)]^{\frac{1}{2}} \tag{3.1.8}$$

Angular frequencies ω_{nm} and ω_{nc} are the real, positive roots of the frequency equation[2]

$$\omega_n^4 - \omega_n^2 [1 + 3\nu - \alpha^2(1 - \nu) + n(n + 1) + \nu\, \alpha^2 n(n + 1)$$

$$+ \alpha^2 n^2 (n + 1)^2] - 2(1 - \nu^2) (1 + \alpha^2) + n(n + 1) (1 - \nu^2)$$

$$+ \alpha^2 n(n + 1) (5 - \nu^2) - 4\, \alpha^2 n^2 (n + 1)^2 + \alpha^2 n^3 (n + 1)^3 = 0 \tag{3.1.9}$$

Solving for twice the square of the frequency yields

$$2\omega_n^2 = 1 + 3\nu - \alpha^2(1 - \nu) + n(n+1) (1+\nu\, \alpha^2) + \alpha^2 n^2 (n+1)^2$$

$$\pm [9 + 6\nu + \nu^2 + 2\, \alpha^2 (3 + \nu) (1 - \nu) + 2n(n+1) (2\nu^2 + 3\nu - 1)$$

$$+ n^2 (n + 1)^2 + 2\, \alpha^2 n(n+1) (5\nu^2 + 2\nu - 11) + 2\, \alpha^2 n^2 (n+1)^2 (9+4\nu)$$

$$- 2\, \alpha^2 n^3 (n+1)^3 - 2\, \alpha^4 n(n+1)\, \nu(1 - \nu) + \alpha^4 n^2 (n+1)^2 (\nu^2 + 2\nu - 2)$$

$$+ 2\nu\, \alpha^4 n^3 (n + 1)^3 + \alpha^4 n^4 (n + 1)^4]^{\frac{1}{2}} \tag{3.1.10}$$

---

2 Equations (3.1.5) are noted to be analogous to a linear, two degree of freedom system; therefore, such roots are known to exist.

The positive sign in (3.1.10) gives the frequency ω_{nm} whereas the negative sign gives ω_{nc}.

Substitution of (3.1.6) into (3.1.2) and (3.1.3) yields the solution of the linear problem, namely

$$\zeta(\xi, \tau) = A_o \operatorname{Sin}(\omega_o\tau + \alpha_o) + \sum_{n=1}^{\infty} [A_{nm} \operatorname{Sin}(\omega_{nm}\tau + \alpha_{nm}) + A_{nc} \operatorname{Sin}(\omega_{nc} \tau + \alpha_{nc})] \; P_n(\operatorname{Cos} \xi) \qquad (3.1.11a)$$

$$\psi(\xi, \tau) = \sum_{n=1}^{\infty} [\delta_{nm}A_{nm}\operatorname{Sin}(\omega_{nm} \tau + \alpha_{nm}) + \delta_{nc}A_{nc}\operatorname{Sin}(\omega_{nc} \tau + \alpha_{nc})] \; \dot{P}_n(\operatorname{Cos} \xi) \qquad (3.1.11b)$$

3.2 Mode Classification

The n=0 mode, pure radial motion with amplitude A_o , is called the breathing mode. Introduction of time by substitution of (2.4.2) into (3.1.8) gives the actual breathing mode angular frequency as

$$\omega_{o_{\text{actual}}} = \frac{1}{a} \left[\frac{2E}{\rho(1 - \nu)} \right]^{\frac{1}{2}} \qquad (3.2.1)$$

a result first derived by Lamb[4].

The distinguishing characteristics of the two mode sets are most readily studied by a quantitative presentation. The frequencies ω_{nm} and ω_{nc} are given in Table 1 for $\nu = .3$, $1 \leq n \leq 10$, and two values of a/h.

Table 1

Angular Frequencies

	ω_{nm}		ω_{nc}	
a/h / n	20	200	20	200
1	1.975	1.974	0	0
2	2.723	2.722	.703	.701
3	3.636	3.635	.841	.830
4	4.598	4.596	.916	.881
5	5.578	5.575	.988	.906
6	6.565	6.562	1.081	.921
7	7.556	7.552	1.206	.931
8	8.550	8.546	1.369	.939
9	9.546	9.541	1.572	.946
10	10.542	10.536	1.813	.954

For all values of a/h the lowest mode frequency is ω_{2c}. This mode is called the fundamental mode.

A striking difference between the ω_{nm} and ω_{nc} mode sets is shown in Table 1. Angular frequencies for ω_{nm} modes are relatively independent of a/h; however, ω_{nc} frequencies are sensitive to changes in a/h. This significant effect suggests a membrane-bending, or extensional-inextensional, mode classification.

For a membrane, or extensional, representation of deformation, first presented by Love[3], no consideration is given to the thickness of the shell. All resistance to deformation is assumed to be provided by stretching of the midsurface. A convenient measure of membrane behavior is the sum of the midsurface strains E_m,

$$E_m = \epsilon_{o\xi} + \epsilon_{o\eta} \tag{3.2.2}$$

For a bending, or inextensional, representation of deformation, first presented by Rayleigh[1], the shell midsurface is assumed to be rigid[3]. E_b, a measure of bending behavior commensurate with E_m, is the sum of the maximum strains occurring in the shell less the sum of the midsurface strains. From (2.3.4) and (2.3.7) the maximum strains occur at $z = h/2$ and their sum is

$$\left(\epsilon_\xi + \epsilon_\eta\right)_{max} = \epsilon_{o\xi} + \epsilon_{o\eta} + \frac{h}{2}\left(1 - \frac{h}{2a}\right)\left\{(1 + \epsilon_{o\xi})\left[\kappa_{o\xi} - \frac{1}{a}\right] + (1 + \epsilon_{o\eta})\left[\kappa_{o\eta}\,\mathrm{Sin}(\phi-\beta) - \frac{1}{a}\right]\right\} \tag{3.2.3}$$

Hence, E_b is given as

$$E_b = \frac{h}{2}\left(1 - \frac{h}{2a}\right)\left\{(1 + \epsilon_{o\xi})\left[\kappa_{o\xi} - \frac{1}{a}\right] + (1+\epsilon_{o\eta})\left[\kappa_{o\eta}\mathrm{Sin}(\phi-\beta) - \frac{1}{a}\right]\right\} \tag{3.2.4}$$

---

3 Midsurface stretching must accompany all deformations of a closed shell (see Love[2], p. 542). Rayleigh was, therefore, able to include only open shells in his inextensional analysis. His limiting case of the opening angle $\rightarrow \Pi$ was physically untenable.

The order of magnitude of E_b is not changed by the neglect of $\epsilon_{o\xi}$, $\epsilon_{o\eta}$, and h/2a with respect to unity. With this,

$$E_b = \frac{h}{2} \left\{ \left[\kappa_{o\xi} - \frac{1}{a} \right] + \left[\kappa_{o\eta} \, \mathrm{Sin}(\phi-\beta) - \frac{1}{a} \right] \right\} \qquad (3.2.5)$$

E_m and E_b are obtained in terms of the displacements ζ and ψ by substitution from (2.5.3). The linearized expressions are

$$E_m = -2\zeta + \psi \, \mathrm{Cot}\, \xi + \dot{\psi} \qquad (3.2.6a)$$

$$E_b = \frac{h}{2a} (2\zeta + \dot{\zeta} \, \mathrm{Cot}\, \xi + \ddot{\zeta}) \qquad (3.2.6b)$$

The ratio $|E_m/E_b|$ is an indicator of mode behavior. A large ratio indicates predominately membrane behavior; a small ratio predominately bending behavior. For every $n \geq 1$ solution (3.1.11) yields the following indicator for modes associated with either ω_{nm} or ω_{nc}:

$$\left| \frac{E_m}{E_b} \right| = \frac{2 + n(n+1)\,\delta_n}{2 - n(n+1)} \cdot \frac{2a}{h} \qquad (3.2.7)$$

in which δ_n is δ_{nm} for an ω_{nm} mode and δ_{nc} for an ω_{nc} mode.

Numerical values of $|E_m/E_b|$ for the ω_{nm} and ω_{nc} mode sets are given in Table 2 for two values of a/h.

Table 2

Mode Indicators

	$\lvert E_m/E_b \rvert$			
	a/h = 20		a/h = 200	
n	ω_{nm}	ω_{nc}	ω_{nm}	ω_{nc}
1	∞	--	∞	--
2	56.4	3.80	564	38.0
3	40.5	2.16	405	21.6
4	36.0	1.32	360	13.2
5	34.1	.88	341	8.8
6	33.2	.64	332	6.4
7	32.5	.48	325	4.8
8	32.0	.36	320	3.6
9	31.8	.28	318	2.8
10	31.7	.24	317	2.4
⋮	⋮	⋮	⋮	⋮
∞	30.8	0	308	0

For a/h = 20 the relatively large values of $\lvert E_m/E_b \rvert$ indicate that the ω_{nm} mode behavior is predominately membrane for all n. However, the indicator values for the same a/h show ω_{nc} modes are both membrane and bending in nature. Their behavior is changed from predominately membrane to predominately bending in the finite range of n's given.

From (3.2.7) the mode indicators are directly proportional to the radius-to-thickness ratio. The value a/h = 20 is about the minimum for a thin shell theory. All indicator values may be made arbitrarily large by increasing a/h, a point emphasized in Table 2 by comparison of a/h = 20 with a/h = 200.

The relatively large values of $|E_m/E_b|$ for ω_{nm} modes at a/h = 20 and their subsequent increase as a/h increases substantiate a membrane mode classification for this set. The corresponding increase of ω_{nc} mode indicators causes the transition from membrane to bending behavior to occur at higher values of n. Conversely, for any n an ω_{nc} mode may be made predominately membrane in behavior by choice of a sufficiently large value of a/h. Classification of the ω_{nc} set as bending modes, as their dependence on a/h suggests, would be equivocal. Therefore, the ω_{nc} modes are classified here as composite modes of vibration.[4]

An extensional treatment of the problem is obtained by setting $\alpha^2 = 0$. Frequency equation (3.1.10) then becomes

---

4 Kalnins[8] studied the modes of vibration by use of strain energy coefficients defined as ratios of bending strain energy to total strain energy. This approach is not unlike that of $|E_m/E_b|$ mode indicators as presented. Modes here classified as composite modes were classified as bending modes and were associated with predominately bending strain energy. This association is dependent on a/h and n as is indicated by (3.2.7) and Table 2, and, therefore, must be qualified. See McIvor and Sonstegard[15].

$$2\,\omega_n^2 = 1 + 3\nu + n(n+1) \pm [9 + 6\nu + \nu^2 + 2n(n+1)\,(2\nu^2 + 3\nu - 1) + n^2(n+1)^2]^{\frac{1}{2}} \qquad (3.2.8)$$

It follows that as $n \to \infty$[5]:

$$\omega_{nm} \to \infty \qquad (3.2.9a)$$

$$\omega_{nc} \to [1 - \nu^2]^{\frac{1}{2}} \qquad (3.2.9b)$$

Membrane mode frequencies increase without bound, as expected. However, composite modes constitute an infinite set in a bounded frequency spectrum, an untenable result.[6] The increasingly membrane behavior of composite modes as a/h increases was noted above. The degeneracy of this set to the paradoxical extensional analysis set is, therefore, not surprising and further substantiates a composite, and not a bending, classification.[7]

---

5 n cannot increase without bound in keeping with the neglect of shear deformation and rotary inertia in this formulation. Consideration of this case is of interest, however, in providing a better understanding of mode characteristics.

6 This is the lower mode set of paradoxical behavior referred to in the Introduction.

7 Association of degenerate " bending " modes with the paradoxical extensional modes was made by Kalnins(8).

The relative independence from a/h of membrane mode frequencies, Table 1, and the results obtained from the extensional formulation indicate that (3.2.8) provides an adequate means for their determination. However, composite mode frequencies may be determined by an extensional analysis only for sufficiently large values of a/h and/or small values of n. Both factors must be considered before use of (3.2.8) is justified.

3.3 Response to an Arbitrary, Symmetric Radial Velocity

A closed spherical shell is suddenly enveloped by a pressure impulse symmetric about a polar axis. For a loading time of sufficiently short duration the result of the impulse is an arbitrary, symmetric initial radial velocity distribution. This velocity distribution is expressed in a series of Legendre polynomials of the first kind as

$$\frac{\partial w}{\partial \tau} = \sum_{n=0}^{\infty} v_n P_n (\text{Cos } \xi) \qquad (3.3.1)$$

where

$$w = a - r$$

Expression (3.3.1) imparts a rigid body translation along the negative polar axis. This motion is eliminated by use of a reference frame with its origin at the shell inertial center moving with an appropriate velocity. This matter is considered in detail in the Appendix. The velocity distribution with respect to the inertial center contributes only to the shell deformation. It is

$$\frac{\partial \tilde{w}}{\partial t} = v_o + \left[v_1 - \frac{1}{4} \sum_{n=1,3,\ldots}^{\infty} v_n S_n \right] P_1 (\text{Cos } \xi)$$

$$+ \sum_{n=2,3,\ldots}^{\infty} v_n P_n (\text{Cos } \xi) \qquad (3.3.2a)$$

$$\frac{\partial \tilde{u}}{\partial t} = \frac{1}{4} \sum_{n=1,3,\ldots}^{\infty} v_n S_n \dot{P}_1 (\text{Cos } \xi) \qquad (3.3.2b)$$

where $\partial\tilde{w}/\partial t$ is the radial velocity distribution, $\partial\tilde{u}/\partial t$ is the meridional velocity distribution and

$$S_n = \frac{(2n)!}{2^{2n}(n!)^2} \left[\frac{4}{4-n^2} + \frac{1}{1} \cdot \frac{n}{2n-1} \cdot \frac{4}{4-(n-2)^2} \right.$$

$$\left. + \frac{1 \cdot 3}{1 \cdot 2} \cdot \frac{n(n-1)}{(2n-1)(2n-3)} \cdot \frac{4}{4-(n-4)^2} + \ldots \right]$$

The brackets contain n + 1 terms.

Motion resulting from the impulse is determined by imposing (3.3.2) as initial conditions on solution (3.1.11). The problem is thus formulated as

$$\zeta(\xi,\tau) = A_o \text{Sin}(\omega_o \tau + \alpha_o) + \sum_{n=1}^{\infty} [A_{nm} \text{Sin}(\omega_{nm} \tau + \alpha_{nm})$$

$$A_{nc} \text{Sin}(\omega_{nc} \tau + \alpha_{nc})] P_n (\text{Cos } \xi) \qquad (3.1.11a)$$

$$\psi(\xi, \tau) = \sum_{n=1}^{\infty} [\delta_{nm} A_{nm} \operatorname{Sin}(\omega_{nm} \tau + \alpha_{nm}) + \delta_{nc} A_{nc} \operatorname{Sin}(\omega_{nc} \tau + \alpha_{nc})] \dot{P}_n(\operatorname{Cos} \xi) \qquad (3.1.11b)$$

$$\zeta(\xi, 0) = 0 \qquad (3.3.3a)$$

$$\psi(\xi, 0) = 0 \qquad (3.3.3b)$$

$$\frac{\partial \zeta}{\partial \tau}(\xi, 0) = \frac{1}{c} \frac{\partial \tilde{w}}{\partial \tau} \qquad (3.3.3c)$$

$$\frac{\partial \psi}{\partial \tau}(\xi, 0) = \frac{1}{ac} \frac{\partial \tilde{u}}{\partial \tau} \qquad (3.3.3d)$$

where

$$c = \left[\frac{E}{\rho(1-\nu^2)} \right]^{\frac{1}{2}}$$

The arbitrary constants in (3.1.11) are now found to be

$$\alpha_o = \alpha_{nm} = \alpha_{nc} = 0 \qquad (3.3.4a)$$

$$A_o = \frac{v_o}{c\omega_o} \qquad (3.3.4b)$$

$$A_{1m} = \frac{v_1 - \frac{1}{4} \sum_{n=1,3,\ldots}^{\infty} v_n S_n}{c\, \omega_{1m}} \qquad (3.3.4c)$$

$$A_{1c} = 0 \qquad (3.3.4d)$$

$$A_{nm} = \frac{\delta_{nc}}{\omega_{nm}(\delta_{nc} - \delta_{nm})} \frac{v_n}{c} \qquad n \geq 2 \qquad (3.3.4e)$$

$$A_{nc} = \frac{\delta_{nm}}{\omega_{nc}(\delta_{nm} - \delta_{nc})} \frac{v_n}{c} \qquad n \geq 2 \qquad (3.3.4f)$$

The solution is of the form

$$\zeta(\xi,\tau) = \Delta_o \text{ Sin } \omega_o\tau + \Delta_{1m}\text{Sin } \omega_{1m}\tau \; P_1(\text{Cos } \xi)$$

$$+ \sum_{n=2}^{\infty} [\Delta_{nm} \text{ Sin } \omega_{nm}\tau + \Delta_{nc}\text{Sin } \omega_{nc}\tau] \; P_n(\text{Cos } \xi) \qquad (3.3.5a)$$

$$\psi(\xi,\tau) = \bar{\Delta}_{1m} \text{ Sin } \omega_{1m}\tau \; \dot{P}_1(\text{Cos } \xi)$$

$$+ \sum_{n=2}^{\infty} [\bar{\Delta}_{nm}\text{Sin}\omega_{nm}\tau + \bar{\Delta}_{nc}\text{Sin}\omega_{nc}\tau] \; \dot{P}_n(\text{Cos } \xi) \qquad (3.3.5b)$$

Δ_{nm} and Δ_{nc} are the radial amplitudes of the nth membrane mode and the nth composite mode respectively. Similarly $\bar{\Delta}_{nm}$ and $\bar{\Delta}_{nc}$ are the meridional amplitudes of the nth membrane mode and nth composite mode respectively. For all $n \geq 2$ the membrane mode radial and meridional amplitudes, Δ_{nm} and $\bar{\Delta}_{nm}$, are compared to the composite mode radial amplitude Δ_{nc}. Then

$$\left|\frac{\Delta_{nm}}{\Delta_{nc}}\right| = \frac{\delta_{nc}\,\omega_{nc}}{\delta_{nm}\,\omega_{nm}} \qquad (3.3.6a)$$

$$\left|\frac{\bar{\Delta}_{nm}}{\Delta_{nc}}\right| = \frac{\delta_{nc}\,\omega_{nc}}{\omega_{nm}} \qquad (3.3.6b)$$

These two amplitude ratios are plotted in Figure 4 for $2 \leq n \leq 10$, $\nu = .3$, and $a/h = 20$. Values shown are negligibly changed for $a/h = 200$.

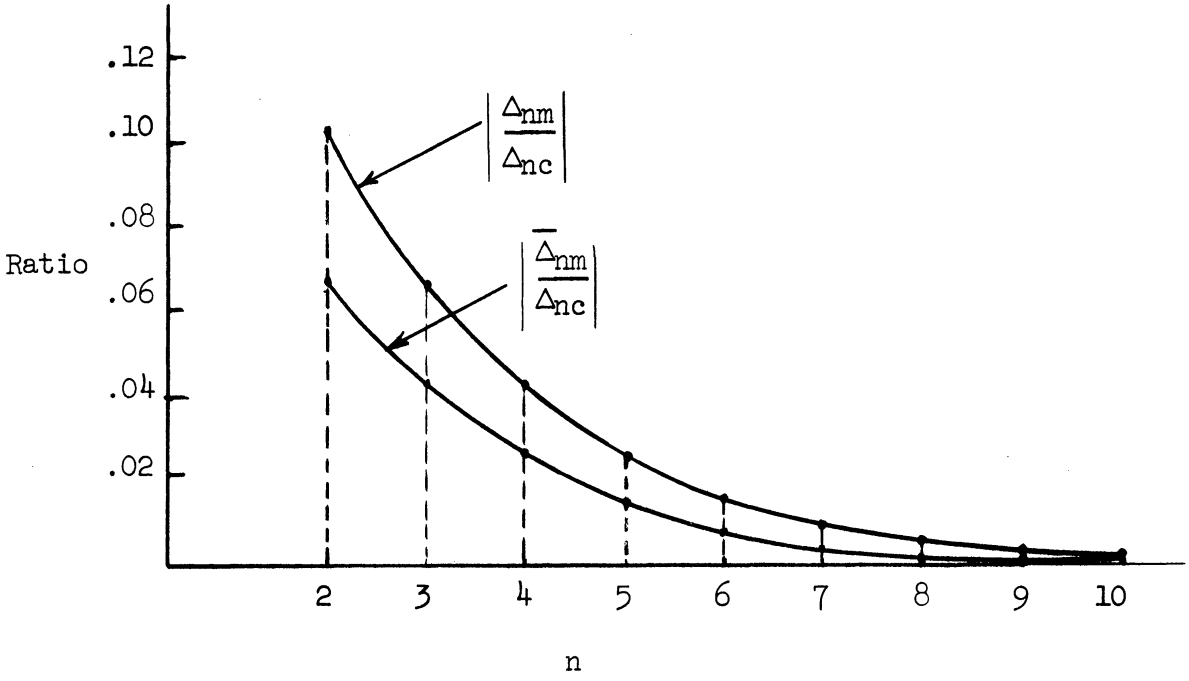

Figure 4. Plot of Amplitude Ratios

Figure 4 indicates that for all appropriate a/h and $n \geq 2$ the motion is predominately due to vibration in composite modes. Hence, it is assumed that the membrane contributions to ζ and ψ for $n \geq 2$ are negligible and that the response to velocity distribution (3.3.2) may be expressed as

$$\zeta(\xi,\tau) = \frac{v_o}{c\omega_o} \operatorname{Sin} \omega_o\tau + \frac{[v_1 - \frac{1}{4} \sum_{n=1,3,\ldots}^{\infty} v_n S_n]}{c\,\omega_{1m}} \operatorname{Sin} \omega_{1m}\tau\, P_1(\operatorname{Cos} \xi)$$

$$+ \sum_{n=2}^{\infty} \frac{v_n}{c\omega_{nc}} \frac{\delta_{nm}}{\delta_{nm} - \delta_{nc}} \operatorname{Sin} \omega_{nc}\tau\, P_n(\operatorname{Cos} \xi) \qquad (3.3.7a)$$

$$\psi(\xi,\tau) = \frac{\frac{1}{4} \sum_{n=1,3,\ldots}^{\infty} v_n S_n}{c\omega_{1m}} \operatorname{Sin} \omega_{1m}\tau\, \dot{P}_1(\operatorname{Cos} \xi)$$

$$+ \sum_{n=2}^{\infty} \frac{v_n}{c\omega_{nc}} \frac{\delta_{nm}\,\delta_{nc}}{\delta_{nm} - \delta_{nc}} \operatorname{Sin} \omega_{nc}\tau\, \dot{P}_n(\operatorname{Cos} \xi) \qquad (3.3.7b)$$

Expressions (3.3.7) do not satify initial conditions (3.3.3) but an approximate set which is

$$\zeta(\xi, 0) = 0 \qquad (3.3.8a)$$

$$\psi(\xi, 0) = 0 \qquad (3.3.8b)$$

$$\frac{\partial \zeta}{\partial \tau}(\xi, 0) = \frac{v_o}{c} + \frac{v_1 - \frac{1}{4} \sum_{n=1,3,\ldots}^{\infty} v_n S_n}{c} P_n(\operatorname{Cos} \xi)$$

$$+ \sum_{n=2}^{\infty} \frac{v_n}{c} \frac{\delta_{nm}}{\delta_{nm} - \delta_{nc}} P_n(\cos \xi) \qquad (3.3.8c)$$

$$\frac{\partial \psi}{\partial \tau}(\xi, 0) = \frac{1}{4} \sum_{\substack{n=1,3,\ldots \\ c}}^{\infty} v_n S_n \, P_1(\cos \xi)$$

$$+ \sum_{n=2}^{\infty} \frac{v_n}{c} \frac{\delta_{nm}\, \delta_{nc}}{\delta_{nm} - \delta_{nc}} \dot{P}_n(\cos \xi) \qquad (3.3.8d)$$

Since ω_{nm} frequencies are higher than the fundamental frequency ω_{2c} (see Table 1) the maximum amplitude of the fundamental mode is attained after those of the membrane modes. Hence, the displacement comparison of Figure 4 is not initially valid and the entire solution (3.3.6) must be retained. The period of the fundamental mode T_f is

$$T_f = \frac{2\Pi}{c\omega_{2c}} \qquad (3.3.9)$$

All composite modes will have attained their maximum amplitudes within a time $\Pi/2c\omega_{2c}$; thereafter, the transition to predominately composite mode deformation will have occurred and approximations (3.3.7) and (3.3.8) may be used.

Since bending effects in the shell are predominately due to composite mode motion an accurate determination of flexural stress may be obtained from the approximate solution. The neglect of membrane mode contributions, however, prohibits determination of membrane stress from this solution.

CHAPTER 4

RESPONSE TO A NEARLY UNIFORM RADIAL IMPULSE

The basic response of a closed spherical shell to a uniform radial impulse is the breathing mode of motion. Small non-uniformities in the impulse may cause this response to be dynamically unstable. The results of Chapter 3 indicate that composite mode deformations will predominate any deviation from the basic response. Breathing mode stability is therefore studied with respect to perturbations of composite modes of motion. Stability criteria are thus determined by the character of nonlinear coupling between linear modes of motion, i.e. by the possibility of autoparametric excitation.

4.1 Formulation

When an uniform impulsive pressure of short duration suddenly envelopes a closed spherical shell, a radial velocity v_o is imparted to every shell element. In terms of the non-dimensional quantities previously introduced the initial conditions are

$$\zeta(\xi, 0) = 0 \tag{4.1.1a}$$

$$\psi(\xi, 0) = 0 \tag{4.1.1b}$$

$$\frac{\partial \zeta}{\partial \tau}(\xi, 0) = \frac{v_o}{c} \tag{4.1.1c}$$

$$\frac{\partial \psi}{\partial \tau}(\xi, 0) = 0 \tag{4.1.1d}$$

where

$$c = \left[\frac{E}{\rho(1 - \nu)^2} \right]^{\frac{1}{2}}$$

Governing equations of motion (2.4.10) and initial conditions (4.1.1) are satisfied by a harmonic breathing mode,

$$\zeta(\xi, \tau) = \frac{v_o}{c\omega_o} \operatorname{Sin} \omega_o \tau \qquad (4.1.2a)$$

$$\psi(\xi, \tau) = 0 \qquad (4.1.2b)$$

where

$$\omega_o = [2(1 + \nu)]^{\frac{1}{2}}$$

If the impulsive pressure is slightly non-uniform, this basic response may be dynamically unstable. This possibility is to be studied by applying an axisymmetric perturbation to the initial velocity, giving initial conditions

$$\zeta(\xi, 0) = 0 \qquad (4.1.3a)$$

$$\psi(\xi, 0) = 0 \qquad (4.1.3b)$$

$$\frac{\partial \zeta}{\partial \tau}(\xi, 0) = \frac{v_o}{c} \left[1 + \sum_{n=1}^{\infty} \epsilon_n P_n(\operatorname{Cos} \xi) \right] \qquad (4.1.3c)$$

$$\frac{\partial \psi}{\partial \tau} (\xi, 0) = 0 \qquad (4.1.3d)$$

where

$$\epsilon_n \ll 1$$

The basic response will be termed stable if the amplitudes of the deviation from the breathing mode remain of the order of magnitude of ϵ_n. Conversely, if these amplitudes grow to magnitudes of higher order, the basic response will be termed unstable.

4.2 The Approximation

An exact solution of nonlinear equations (2.4.10) satisfying initial conditions (4.1.3) has not been found. An approximation is feasible by utilizing results of Chapter 3.

The perturbation in the uniform initial velocity, equations (4.1.3), constitutes initial conditions for the response to an arbitrary, symmetric radial velocity distribution, equations (3.3.2). From Section 3.3 the corresponding linear response is predominately composite mode motion. This result is extended to the slightly larger motions anticipated here. The perturbation of the basic response is limited to a superposition of composite mode motion on the breathing mode. The investigation is thus a study of the stability of the breathing mode with respect to composite mode deviation only.

An approximate set of initial conditions is now formulated. Conditions (4.1.3) are expressed in the form of (3.3.8) as

$$\zeta(\xi, 0) = 0 \tag{4.2.1a}$$

$$\psi(\xi, 0) = 0 \tag{4.2.1b}$$

$$\frac{\partial \zeta}{\partial \tau}(\xi, 0) = \frac{v_o}{c}\left[1 + (\epsilon_1 + \bar{\epsilon})\, P_1(\cos \xi) + \sum_{n=2}^{\infty} \epsilon_n P_n(\cos \xi)\right] \tag{4.2.1c}$$

$$\frac{\partial \psi}{\partial \tau}(\xi, 0) = \frac{v_o}{c}\left[\bar{\epsilon}\, \dot{P}_1(\cos \xi) + \sum_{n=2}^{\infty} \epsilon_n \delta_{nc} \dot{P}_n(\cos \xi)\right] \tag{4.2.1d}$$

The quantity $\bar{\epsilon}$ represents the effect of having chosen a reference system so as to remove rigid body motion imparted by (4.1.3). $\bar{\epsilon}$ may be determined by the method outlined in the Appendix. The contribution of $\bar{\epsilon}$ to the response will be of an order of magnitude of a perturbation and is neglected. The approximation implies a perturbation free of a first mode (membrane) component; hence, ϵ_1 is also neglected. The resulting initial conditions are

$$\zeta(\xi, 0) = 0 \tag{4.2.2a}$$

$$\psi(\xi, 0) = 0 \tag{4.2.2b}$$

$$\frac{\partial \zeta}{\partial \tau}(\xi, 0) = \frac{v_o}{c}\left[1 + \sum_{n=2}^{\infty} \epsilon_n P_n(\text{Cos } \xi)\right] \qquad (4.2.2c)$$

$$\frac{\partial \psi}{\partial \tau}(\xi, 0) = \frac{v_o}{c} \sum_{n=2}^{\infty} \epsilon_n \delta_{nc} \dot{P}_n(\text{Cos } \xi) \qquad (4.2.2d)$$

The assumed solution consists of the breathing mode together with composite modes. From equations (3.3.7) the appropriate representation is

$$\zeta(\xi, \tau) = a_o(\tau) + \sum_{n=2}^{\infty} a_n(\tau)\, P_n(\text{Cos } \xi) \qquad (4.2.3a)$$

$$\psi(\xi, \tau) = \sum_{n=2}^{\infty} a_n(\tau)\, \delta_{nc}\, \dot{P}_n(\text{Cos } \xi) \qquad (4.2.3b)$$

4.3 Stability of the Breathing Mode

The approximation of Section 4.2 allows a study of the stability of the breathing mode using the energy formulation of Section 2.4.

The Lagrangian L is (2.4.3) minus (2.4.7). The neglect of 2ζ with respect to unity gives

$$L = \frac{\Pi\, a^2 E\, h}{1 - \nu^2} \int_0^{\Pi} \left\{ \left(\frac{\partial \zeta}{\partial \tau}\right)^2 + \left(\frac{\partial \psi}{\partial \tau}\right)^2 - \dot{\psi}^2 - \psi^2 \text{Cot}^2 \xi \right.$$

$$- 2(1 + \nu)\,(\zeta^2 - \zeta\psi\, \text{Cot } \xi - \zeta\dot{\psi} + \zeta^2\psi\, \text{Cot } \xi + \zeta^2\dot{\psi})$$

$$+ 2\zeta\dot{\psi}^2 - \dot{\zeta}^2\dot{\psi} + \zeta\, \dot{\zeta}^2 - \zeta\psi^2 + \psi^3 \text{Cot } \xi + 2\, \zeta\, \psi^2 \text{Cot}^2 \xi$$

$$\left. - 2\nu(\psi\, \dot{\psi}\, \text{Cot } \xi - \tfrac{1}{2}\, \psi^2\dot{\psi} - 2\, \zeta\psi\dot{\psi}\, \text{Cot } \xi + \tfrac{1}{2}\, \zeta\psi^2 - \tfrac{1}{2}\, \zeta\, \dot{\zeta}^2 \right.$$

$$+ \tfrac{1}{2}\,\dot{\xi}^2\psi\ \mathrm{Cot}\ \xi) - \alpha^2[\dot{\psi}^2 + \psi^2\mathrm{Cot}^2\xi + 2\,\ddot{\xi}\,\dot{\psi} + 2\,\dot{\xi}\,\psi\ \mathrm{Cot}^2\xi$$

$$+ \ddot{\xi}^2 + \dot{\xi}^2\mathrm{Cot}^2\xi + 2\nu(\psi\,\dot{\psi}\ \mathrm{Cot}\ \xi + \dot{\xi}\,\dot{\psi}\ \mathrm{Cot}\ \xi$$

$$+ \ddot{\xi}\,\psi\ \mathrm{Cot}\ \xi + \dot{\xi}\,\ddot{\xi}\ \mathrm{Cot}\ \xi]\Big\}\ \mathrm{Sin}\ \xi\ d\ \xi \qquad (4.3.1)$$

Representation (4.2.3) is now substituted into the Lagrangian. Initially $a_n (n \geq 2)$ is of an order of magnitude of a perturbation, i.e. $a_n \ll a_o$. Lagrangian terms of order three will therefore be retained only if a_o occurs to at least the first power. After integration the Lagrangian valid for initial motion may be expressed

$$L = \frac{\Pi\, a^2 E\, h}{1-\nu^2}\Bigg\langle 2\left(\frac{Da_o}{D\tau}\right)^2 + 2\sum_{n=2}^{\infty}\frac{\left(\frac{Da_n}{D\tau}\right)^2}{2n+1}[1 + \delta_{nc}^2 n(n+1)]$$

$$- 2\sum_{n=2}^{\infty}\frac{\delta_{nc}^2 a_n^2}{2n+1}\, n(n+1)\,[n(n+1) - 1 + \nu]$$

$$- 4(1+\nu)\left\{a_o^2 + \sum_{n=2}^{\infty}\frac{a_n^2}{2n+1}\,[1 + \delta_{nc} n(n+1)]\right\}$$

$$- 2\alpha^2\sum_{n=2}^{\infty}\frac{a_n^2}{2n+1}\,(1+\delta_{nc})^2\, n(n+1)\,[n(n+1) - 1 + \nu]$$

$$+ 8(1+\nu)\, a_o \sum_{n=2}^{\infty}\frac{\delta_{nc}\, a_n^2}{2n+1}\, n(n+1)$$

$$+ 4\, a_o \sum_{n=2}^{\infty} \frac{\delta_{nc}^2\, a_n^2}{2n+1}\, n(n+1)\,[n(n+1) - 1 + \nu]$$

$$+ 2(1+\nu)\, a_o \sum_{n=2}^{\infty} \frac{a_n^2}{2n+1}\, n(n+1)\,(1 - \delta_{nc}^2) \Big\rangle \qquad (4.3.2)$$

Quantities a_o and a_n $(n \geq 2)$ are identified as generalized coordinates. Motion is, therefore, governed by Lagrange's equations expressed as

$$\frac{D}{D\tau}\left[\frac{\partial L}{\partial\left(\frac{Da_o}{D\tau}\right)}\right] - \frac{\partial L}{\partial a_o} = 0 \qquad (4.3.3a)$$

$$\frac{D}{D\tau}\left[\frac{\partial L}{\partial\left(\frac{Da_n}{D\tau}\right)}\right] - \frac{\partial L}{\partial a_n} = 0 \qquad n \geq 2 \qquad (4.3.3b)$$

Introducing L from (4.3.2) into (4.3.3) yields the equations governing initial motion. They are

$$\frac{D^2 a_o}{D\tau^2} + 2(1+\nu)\, a_o - \sum_{n=2}^{\infty} \frac{a_n^2}{2n+1}\, n(n+1) \left\{ \frac{1+\nu}{2} \right.$$

$$\left. + 2\,\delta_{nc}(1+\nu) + \delta_{nc}^2\left[n(n+1) - \frac{3-\nu}{2}\right] \right\} = 0 \qquad (4.3.4a)$$

$$\frac{D^2 a_n}{D\tau^2}\left[1 + \delta_{nc}^2\, n(n+1)\right] + \left\{ 2(1+\nu)\left[1 + \delta_{nc}\, n(n+1)\right] \right.$$

$$+ n(n+1)\,[n(n+1) - 1 + \nu]\,[\delta_{nc}^2 + \alpha^2(1+\delta_{nc})^2]\Big\}\, a_n$$

$$-\Big\{(1-\delta_{nc}^2)\, n(n+1)\,(1+\nu) + 2\,\delta_{nc}^2\, n(n+1)\,[n(n+1) - 1+\nu]$$

$$+ 4\,\delta_{nc}(1+\nu)\, n(n+1)\Big\}\, a_o a_n = 0 \qquad n \geq 2 \qquad (4.3.4b)$$

Since $a_n^2 \ll a_o$ initially, equation (4.3.4a) may be rewritten as

$$\frac{D^2 a_o}{D\tau^2} + 2(1+\nu)\, a_o = 0 \qquad (4.3.5)$$

the solution of which is the breathing mode motion

$$a_o = \frac{v_o}{c\omega_o} \operatorname{Sin}\ \omega_o \tau \qquad (4.3.6)$$

The constants of integration have been evaluated for initial conditions following from (4.2.2) and (4.2.3a).

Solution (4.3.6) is now substituted into (4.3.4b). A change of independent variable

$$\bar{\tau} = \omega_o \tau$$

gives

$$\frac{D^2 a_n}{D\bar{\tau}^2} + (\Omega_n - \mu_n \operatorname{Sin} \bar{\tau})\, a_n = 0 \quad n \geq 2 \qquad (4.3.7)$$

where

$$\Omega_n = \frac{1}{\omega_0^2[1+\delta_{nc}^2\, n(n+1)]} \left\{ 2(1+\nu)[1 + \delta_{nc}\, n(n+1)] \right.$$

$$\left. + n(n+1)\,[n(n+1) - 1 + \nu]\,[\delta_{nc}^2 + \alpha^2(1 + \delta_{nc})^2] \right\} \qquad (4.3.8a)$$

$$\mu_n = \frac{v_o}{c\omega_0^3} \frac{1}{1+\delta_{nc}^2\, n(n+1)} \left\{ (1 - \delta_{nc}^2)\, n(n+1)\,(1+\nu) \right.$$

$$+ 2\,\delta_{nc}^2\, n(n+1)\,[n(n+1) - 1+\nu]$$

$$\left. + 4\,\delta_{nc}\,(1+\nu)\, n(n+1) \right\} \qquad (4.3.8b)$$

Equation (4.3.8a) may also be expressed as

$$\Omega_n = \frac{\omega_{nc}^2}{\omega_0^2} \qquad (4.3.9)$$

thereby emphasizing the character of (4.3.4b). The linear portion of the equations represents motion in composite modes of vibration. The non-linear, or $a_o\, a_n$ terms represent coupling of the breathing mode with composite modes.

Equations (4.3.7) are Mathieu equations. Thus deviations from the breathing mode are Mathieu functions and their growth characteristics

are determined from the well known Mathieu stability diagram shown in Figure 5 (see, for example, Stoker[16] p. 202)[1].

Whether or not a particular deviation amplitude a_n remains of an order of magnitude of a perturbation is readily deduced by location of the point (Ω_n, μ_n) on Figure 5. If the point falls in an unshaded region or on a boundary curve other than $\mu_n = 0$, the amplitude a_n will increase exponentially and the breathing mode is unstable. Such a deviation will be called a critical deviation[2]. Otherwise a_n will not change order of magnitude and the breathing mode is stable.

The two bounding curves for a particular unstable region intersect the positive Ω axis at $\Omega = k^2/4$ $(k = 1,2,3,...)$. In the discussion to follow a region will be denoted by this intersection, such as region .25.

---

1 Breathing mode stability for the cylindrical shell was also found to be governed by Mathieu equations by Goodier and McIvor[13]. Their study includes analog computor results which demonstrate the stable and unstable growth characteristics of Mathieu functions. These results will not be reproduced.

2 Floquet theory, see Stoker[16] p. 193, predicts that a critical deviation will grow without bound, an impossible consequence for the fixed, finite energy input of the initial pulse. Terms in (4.3.4) predominating after growth starts have been neglected. Their effect is examined in Section 4.4.

The membrane stress generated by the breathing mode is

$$\sigma_o = \frac{E}{1 - \nu} \cdot \frac{v_o}{c\omega_o} \text{ Sin } \omega_o \tau \qquad (4.3.10)$$

For the material to remain elastic, σ_o must remain less than the yield stress. Thus for a material of yield stress σ_y the maximum radial velocity imparted by the initial pulse may be expressed as

$$\left(\frac{v_o}{c}\right)_{max} = \frac{\sigma_y}{E} \omega_o (1 - \nu) \qquad (4.3.11)$$

About the largest σ_y/E value of practical interest is $5(10)^{-3}$. The maximum value of v_o/c for this case is denoted V_{max} and is

$$V_{max} = 5.646 (10)^{-3} \qquad (4.3.12)$$

A pertinent portion of the Mathieu stability diagram for V_{max} is shown in Figure 6. The a/h curves have significance only at intersections with the dashed, nearly horizontal lines denoting integer values of n. Those intersections occurring in unshaded regions or on their boundaries indicate deviation growth and breathing mode instability.

For example, for a shell of a/h = 100 intersections occur in region 1.0 at n = 21 and 22. Deviation amplitudes a_{21} and a_{22} therefore increase exponentially and the breathing mode is unstable. For a/h = 50 no intersections occur in an unshaded region or on a boundary

and the breathing mode is stable. By interpolation between curves, a_{12} will cause instability at about $a/h = 35$. It is notable that no instability can occur for $n \leq 9$, $a/h \geq 20$.

In Figure 6 critical deviations occur in region .25 for sufficiently large a/h. At $a/h = 150$ deviations 11 through 17 will cause breathing mode instability (other critical deviations occur outside region .25, a matter to be discussed later). More and more critical deviations are included in region .25 as a/h is increased.

Referring now to Figure 5, regions 1.0,2.25,... become increasingly narrow strips for decreasing μ. Should a point $(\hat{\Omega}_n , \hat{\mu}_n)$ fall within such a strip an unstable solution is indicated. The corresponding deviation is not classified as critical, however, because an unjustifiably precise knowledge of the system constants is presumed in order to locate $(\hat{\Omega}_n, \hat{\mu}_n)$. Furthermore, the inevitable presence of damping cuts off portions of the unstable regions which border on the Ω axis, see Bolotin[12], § 9. From Figure 6 it is clear, however, that critical deviations may occur in regions 1.0,2.25,... for sufficiently high n and large values of a/h. Therefore, as a/h increases consideration must be given to occurance of critical deviations in more and more regions.

Lubkin and Stoker[17] showed that in the presence of an arbitrarily small amount of damping a value Ω_o exists for which the region $\Omega > \Omega_o$, $\mu < \Omega$ is entirely stable. For large n,

$$\frac{\mu_n}{\Omega_n} \rightarrow \frac{v_o}{c\omega_o} \frac{1}{\alpha^2 n^2} \qquad (4.3.12)$$

Hence, for all a/h (expect the extensional case) some n exists above which critical deviations will not occur.

It is interesting to note that the Mathieu diagram, Figure 5, is symmetric about the Ω axis. Consequently the stability criteria for an inward initial velocity remain unchanged for an outward initial velocity.

The stability diagram for .6 V_{max} , or, what is equivalent, for the maximum value of v_o/c when $\sigma_y/E = 3(10)^{-3}$, is shown in Figure 7. The effect of this reduced initial velocity is apparent from comparison of Figures 6 and 7. Since Ω_n is independent of v_o/c, the ordinate μ_n of all points is simply multiplied by the factor .6. The stability diagram for any other v_o/c may be determined accordingly.

Referring to examples given on p.44 for Figure 6, reduction of V_{max} by .6 leaves only a_{21} as a critical deviation at a/h = 100. a/h = 50 still gives a stable breathing mode. a_{12} will no longer give instability for any value of a/h; in fact, no critical deviations can now occur for $n \leq 14$. As before, consideration of region .25 and of the portion of regions 2.25,... with significant width is necessary for correspondingly higher a/h and n.

Two striking characteristics of stability behavior are noted in Figures 6 and 7. The first is that relatively high order modes are excited. At V_{max} , $\sigma_y/E = 5(10)^{-3}$, no modes of order less than 10 cause instability. For smaller values of σ_y/E this lower limit is increased. The second is that for thinner shells instability will almost always occur.

4.4 Long-term Behavior

The Mathieu equations governing breathing mode stability are valid only for initial motion. Only those third order terms containing a_o to at least the first power were retained in Lagrangian expression (4.3.2). As indicated on p. 43, terms must be added to this expression after deviation growth starts or a paradoxical energy buildup will occur.

The ratio of meridional to radial displacements δ_{nc} is much less than unity for the composite modes which may be strongly excited. Significant third order contributions to the Lagrangian (4.3.1) are thus assumed to come solely from the term $(1 + \nu)\, \zeta\, \dot{\zeta}^2$ since all other such terms contain ψ and/or $\dot{\psi}$.

Using representation (4.2.2), the Lagrangian is now given by (4.3.2) plus the term

$$\frac{\Pi\, a^2 E\, h}{1-\nu^2} \left\langle (1+\nu) \int_{-1}^{+1} \left[\sum_{n=2}^{\infty} a_n P_n(x) \right] \left[\sum_{m=2}^{\infty} a_m P_m^1(x) \right]^2 dx \right\rangle \qquad (4.4.1)$$

Subsequent substitution into Lagrange's equations gives

$$\frac{D^2 a_o}{D\tau^2} + \omega_o^2 a_o - \frac{1+\nu}{2} \sum_{n=2}^{\infty} \frac{n(n+1)}{2n+1} a_n^2 = 0 \qquad (4.4.2a)$$

$$\frac{D^2 a_n}{D\tau^2} + \omega_o^2 \left[\Omega_n - \frac{c\omega_o}{v_o} \mu_n a_o \right] a_n$$

$$- (1+\nu) \frac{\partial}{\partial a_n} \left\{ \int_{-1}^{+1} \left[\sum_{m=2}^{\infty} a_m P_m(x) \right] \left[\sum_{q=2}^{\infty} a_q P_q^1(x) \right]^2 dx \right\} = 0 \qquad (4.4.2b)$$

The last term in each of equations (4.4.2) is significant only for those n denoting critical deviations. In (4.4.2a) this term gives a reduction of breathing mode amplitudes as deviations grow. This term, containing the integral, in (4.4.2b) will give two forms of contributions. The first form will contain products of the a's with equal subscripts; the second will contain products with unequal subscripts. The latter form represents interactions between critical deviations.

The relatively high orders of Legendre polynomials involved prohibit the practical evaluation of the integral term in (4.4.2b). The effect of this term has been determined at V_{max} for one critical deviation, a_{10}, and at 1.4 V_{max} for two critical deviations, a_9 and a_{10}. The numerical solutions of (4.4.2) showed the integral term to be of negligible consequence in these cases.[3]

---

3 Since the solutions are qualitatively similar to other cases to be presented later they are not pursued in detail.

This observation lends credence to an approximation which facilitates the study of long-term behavior for higher values of n. It is assumed that the second order terms which would result from the retention of the integral expression are negligible with respect to the linear term $\omega_o^2 \Omega_n a_n$.

The resulting equations governing long-term motion,

$$\frac{D^2 a_o}{D\tau^2} + \omega_o^2 a_o - \frac{1+\nu}{2} \sum_{n=2}^{\infty} \frac{n(n+1)}{2n+1} a_n^2 = 0 \qquad (4.4.3a)$$

$$\frac{D^2 a_n}{D\tau^2} + \omega_o^2 \left[\Omega_n - \frac{c\omega_o}{v_o} \mu_n a_o \right] a_n = 0 \qquad (4.4.3b)$$

have been solved numerically for several cases of instability.

A representative long-term behavior is shown in Figure 8 for $a/h = 100$, $v_o/c = V_{max}$. Critical deviations 21 and 22 grow in amplitude, as was predicted in Figure 6, and are seen to enter a cyclic energy exchange with the breathing mode.

The results for a reduced impulse of .6 V_{max} is shown in Figure 9. As predicted in Figure 7, only deviation 21 is critical and again a cyclic energy exchange with the breathing mode is observed.

An interesting feature of the energy exchanges which was observed in all solutions obtained is demonstrated in Figures 6 through 9. From Figure 8, the time required for energy exchange to occur with a_{22} is less

than that with a_{21} . By comparison of Figures 8 and 9, the time required for exchange with a_{21} is significantly increased for the reduced impulse .6 V_{max}. Noting the corresponding positions of these deviations on the stability diagrams, Figures 6 and 7, it is observed that the time required for significant amplitude growth is less for increased μ_n and for increased distance from the boundaries of the instability regions.

The extent to which energy is transferred from the breathing mode to critical deviations is of considerable interest. The total energy T_i imparted to the shell by the impulsive pressure is

$$T_i = 2\Pi\, a^2 \rho\, h\, v_o^2 \qquad (4.4.4)$$

The potential, or strain, energy stored in the shell at any time τ is

$$V = \frac{2\Pi\, a^2 E\, h\, \omega_o^2}{1 - \nu^2} \left[a_o^2 + \sum_{n=2}^{\infty} \frac{1}{2n+1} \left(\Omega_n a_n^2 - \frac{c\omega_o}{v_o} \mu_n a_o a_n^2 \right) \right] \qquad (4.4.5)$$

In (4.4.5) the terms corresponding to the second order terms neglected in (4.4.3) have been deleted. Should all the energy be contained in critical deviation N, the potential energy at some time will be

$$V_N = \frac{2\Pi a^2 E h\, \omega_o^2}{1-\nu^2} \frac{\Omega_N}{2N+1} a_N^2 \qquad (4.4.6)$$

Equating V_N to T_i gives the deviation amplitude A_N for complete energy exchange. It is

$$A_N = \left[\frac{2N + 1}{\Omega_N}\right]^{\frac{1}{2}} \cdot \frac{v_o}{c\omega_o} \tag{4.4.7}$$

For N = 22 and V_{max} ,

$$A_{22} = 6.25 \left(\frac{v_o}{c\omega_o}\right) \tag{4.4.8}$$

For N = 21 and .6 V_{max} ,

$$A_{21} = 6.49 \left(\frac{v_o}{c\omega_o}\right) \tag{4.4.9}$$

From the maximum deviation amplitudes attained in Figures 8 and 9 it is concluded that the energy exchanges are essentially complete. In Figure 8 the different time intervals for deviation growths result in a significant energy content in but one deviation at some instant. In both Figures 8 and 9 the amplitude a_o of the breathing mode is seemingly significant at times of essentially complete energy exchange. Its energy content is, however, small. The total energy was calculated as a check at each step of the numerical analysis. The energy content of the system remained constant and thus the terms neglected in the approximation do not significantly contribute to the total energy.

The sum of the maximum flexural stresses in a case of complete energy transfer is

$$(\sigma_\xi + \sigma_\eta)_{flex} = \frac{E}{1-\nu} \cdot \frac{h}{2a} \left[N(N+1) - 2\right] A_N \qquad (4.4.10)$$

By substitution from (4.4.7),

$$(\sigma_\xi + \sigma_\eta)_{flex} = \frac{E}{1-\nu} \frac{h}{2a} \left[N(N+1) - 2\right] \left[\frac{2N+1}{\Omega_N}\right]^{\frac{1}{2}} \frac{v_o}{c\omega_o} \qquad (4.4.11)$$

In terms of σ_o, the stress produced by the basic breathing mode, (4.4.11) becomes

$$(\sigma_\xi + \sigma_\eta)_{flex} = \frac{h}{2a} \left[N(N+1) - 2\right] \left[\frac{2N+1}{\Omega_N}\right]^{\frac{1}{2}} \sigma_o \qquad (4.4.12)$$

For the two examples of essentially complete energy exchange given above it follows that

$$\left[(\sigma_\xi + \sigma_\eta)_{flex}\right]_{N=22} = 15.75\ \sigma_o \qquad (4.4.13a)$$

$$\left[(\sigma_\xi + \sigma_\eta)_{flex}\right]_{N=21} = 14.38\ \sigma_o \qquad (4.4.13b)$$

Hence, the stresses caused by breathing mode instability may be considerably in excess of those predicted by consideration of the breathing mode alone.

The neglect of higher order terms in (4.4.2) limits numerical consideration of long-term behavior. The limitation may be observed in the potential energy expression (4.4.5). For sufficiently small Ω_n and large μ_n this expression may become negative, a physically untenable result. Such was the case in attempted numerical solutions for V_{max}, $a/h \geq 150$, i.e. as modes grow the contributions of the integral term in (4.4.2b) become significant. However, for all these attempted solutions the deviation growth was initially as predicted by the Mathieu stability diagram and the time required for significant growth was again characterized by the location of the deviation with respect to μ_n and the bordering curves.

4.5 Conclusions

The closed spherical shell under nearly uniform axisymmetric impulsive loading may undergo autoparametric excitation. The parametric effect is generated by nonlinear coupling between the breathing mode and certain composite modes of motion, i.e. by the interaction of the membrane stress with the flexural curvature.

The breathing mode seldom excites relatively low order composite modes. High order modes are almost always excited for thinner shells.

In those cases of long-term behavior for which numerical solutions have been obtained an essentially complete, cyclic energy exchange occurs between the breathing mode and the parametrically excited modes. Resulting displacements and stresses are in excess of those predicted by a consideration of the breathing mode response only.

A thorough numerical study of long-term behaviors for very thin shells ($a/h \geq 150$) has not been made. This limitation is due to extensive computation required in the evaluation of an integral expression involving relatively high order Legendre polynomials. Initial behavior for these cases is not affected by the limitation; therefore, the same general conclusions are implied although quantitative results are not available.

Further pursuit of long-term behavior for very thin shells does not seem appropriate for this axisymmetric formulation. A realistic appraisal of the physical situation for the relatively large values of n entailed for such shells indicates that asymmetric effects would be significant.

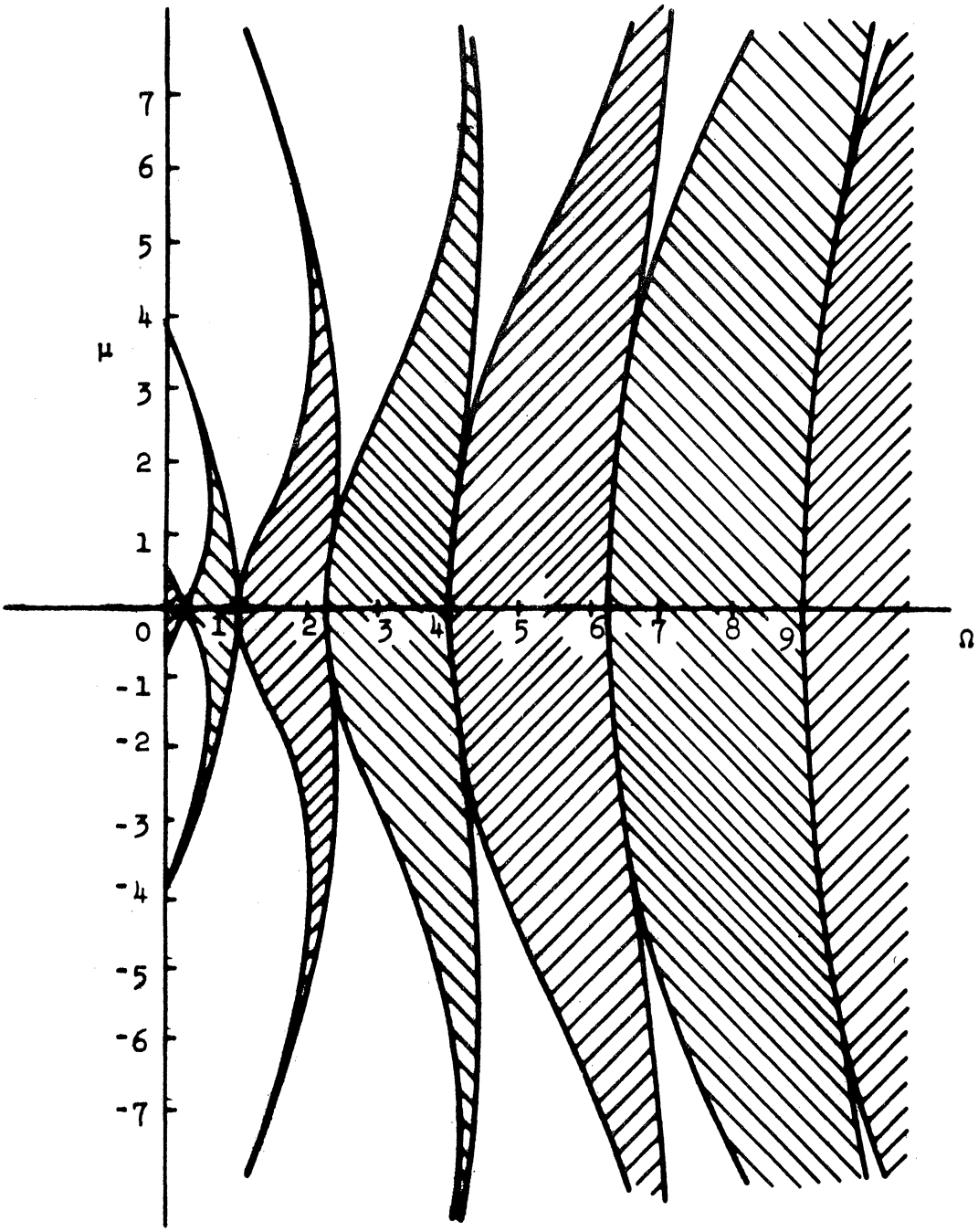

Figure 5. Mathieu Stability Diagram

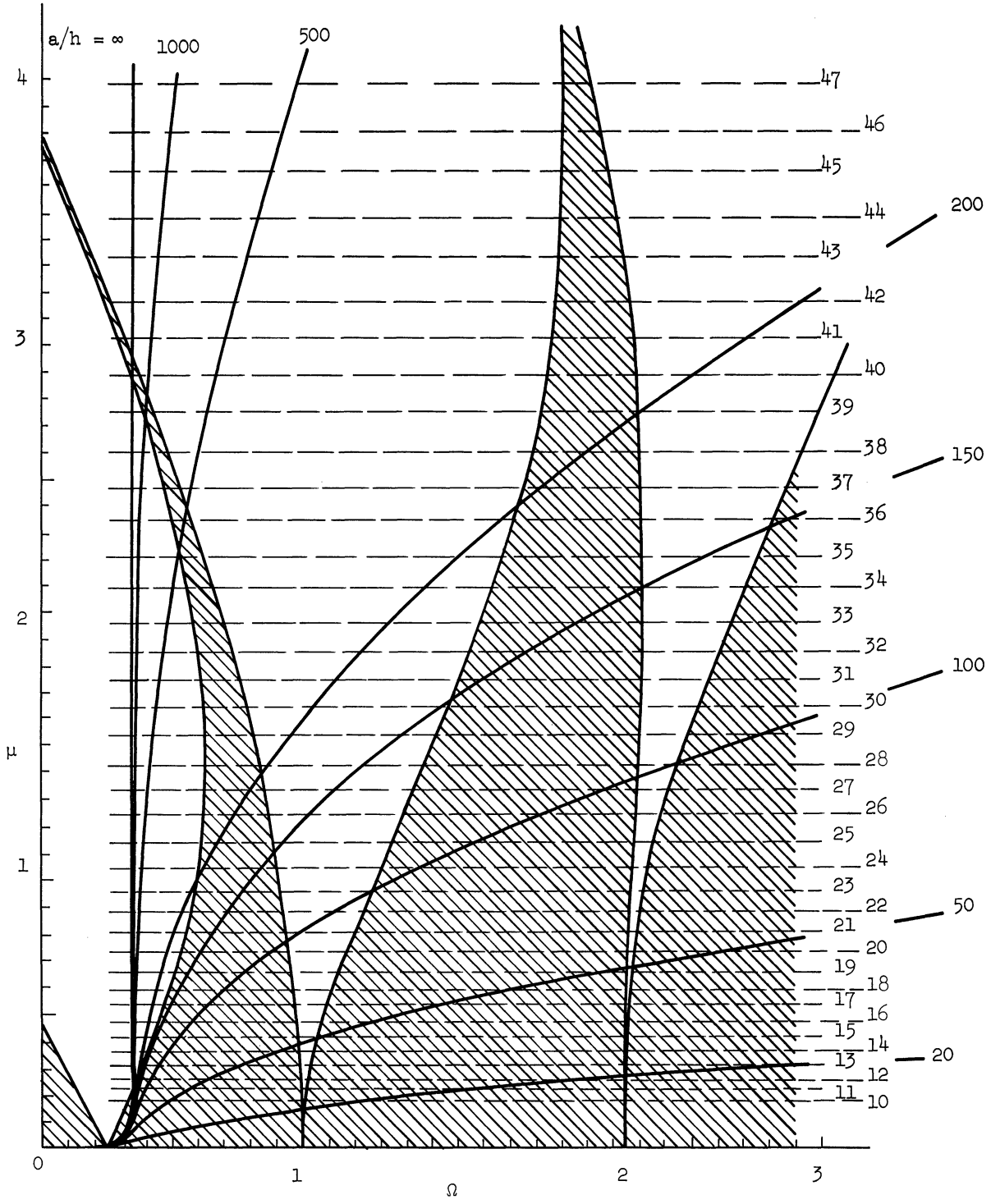

Figure 6. Stability Diagram for V_{max}

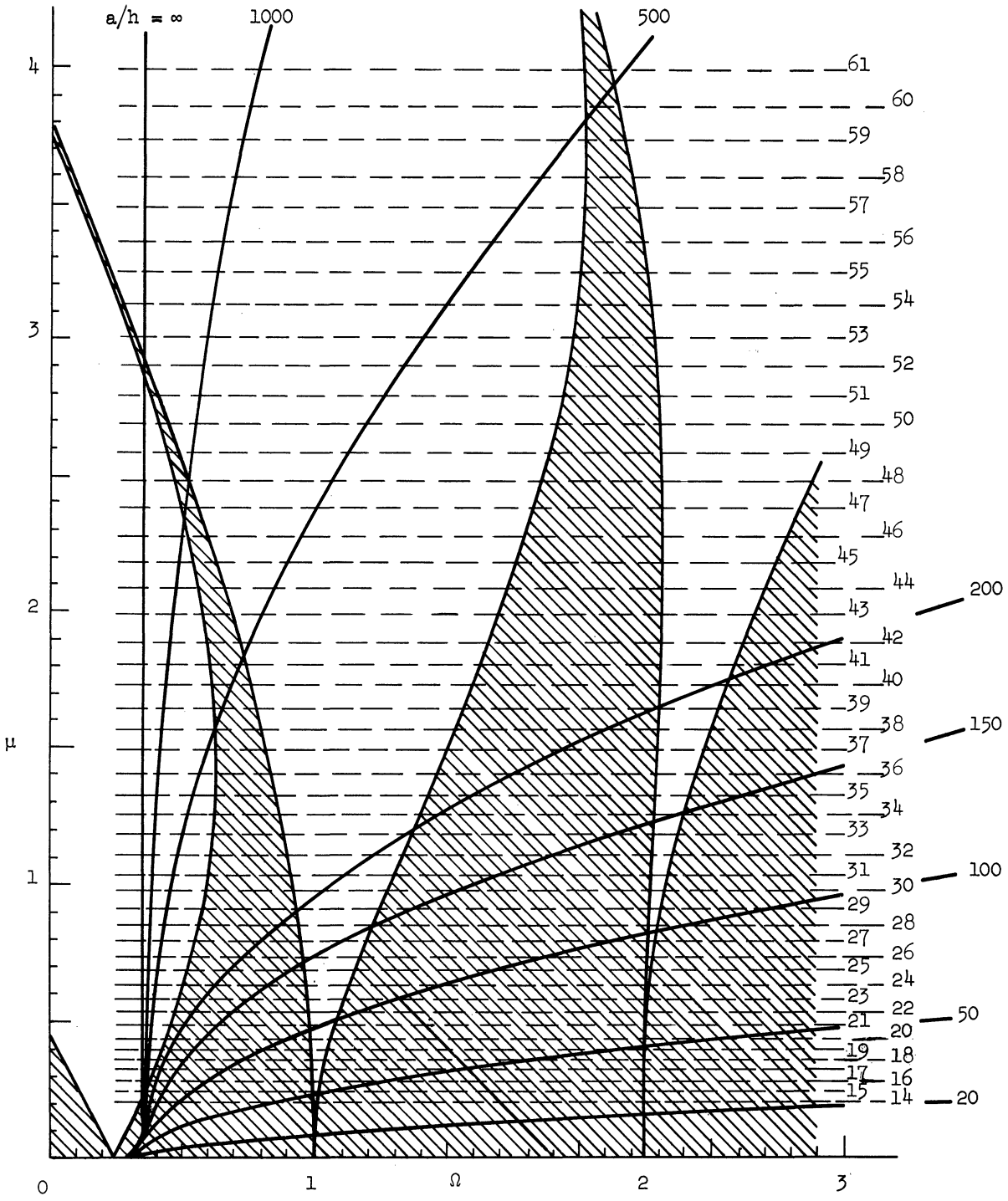

Figure 7. Stability Diagram for .6 V_{max}

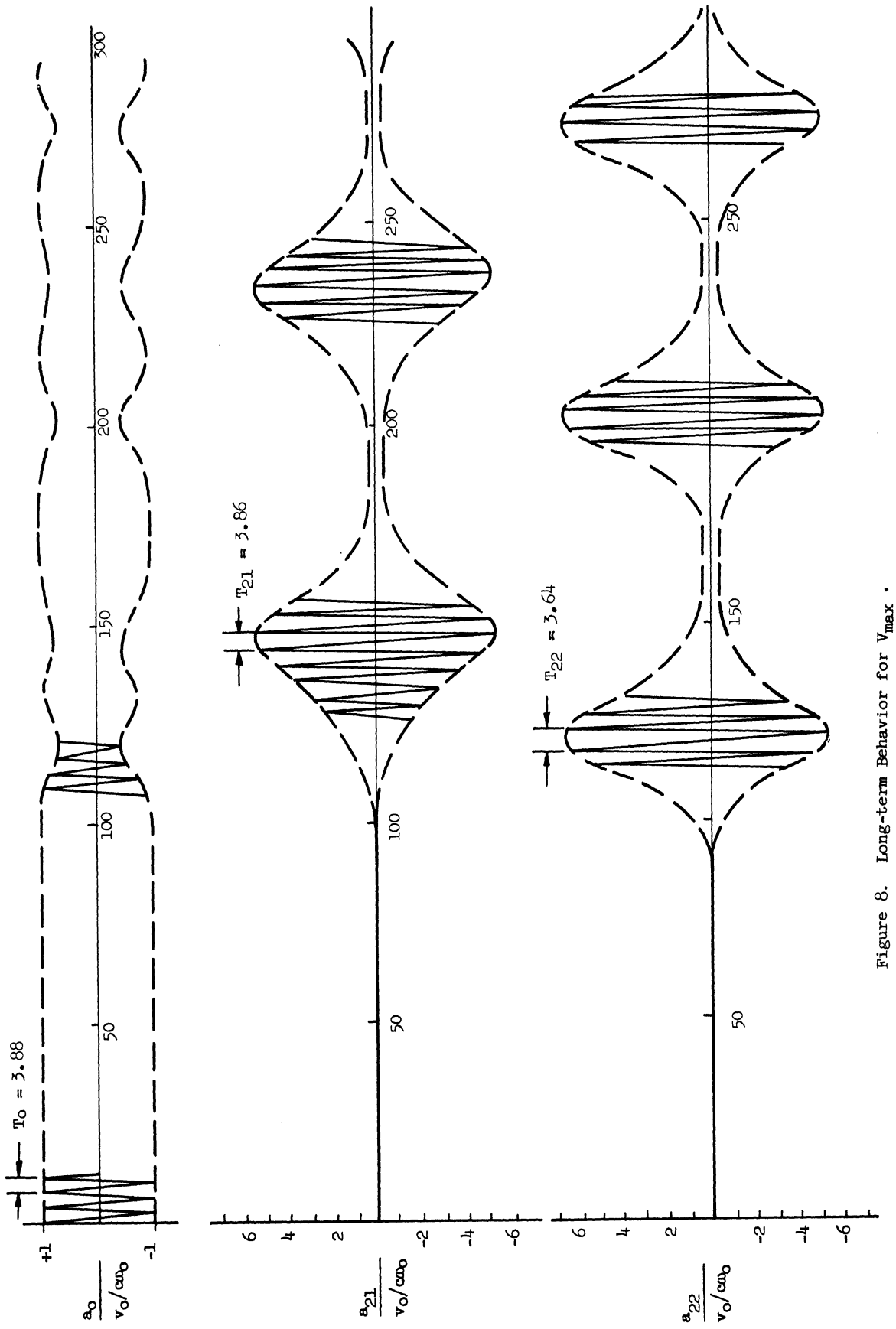

Figure 8. Long-term Behavior for V_{max} .
$a/h = 100$, $\epsilon_n = .05/n^3$

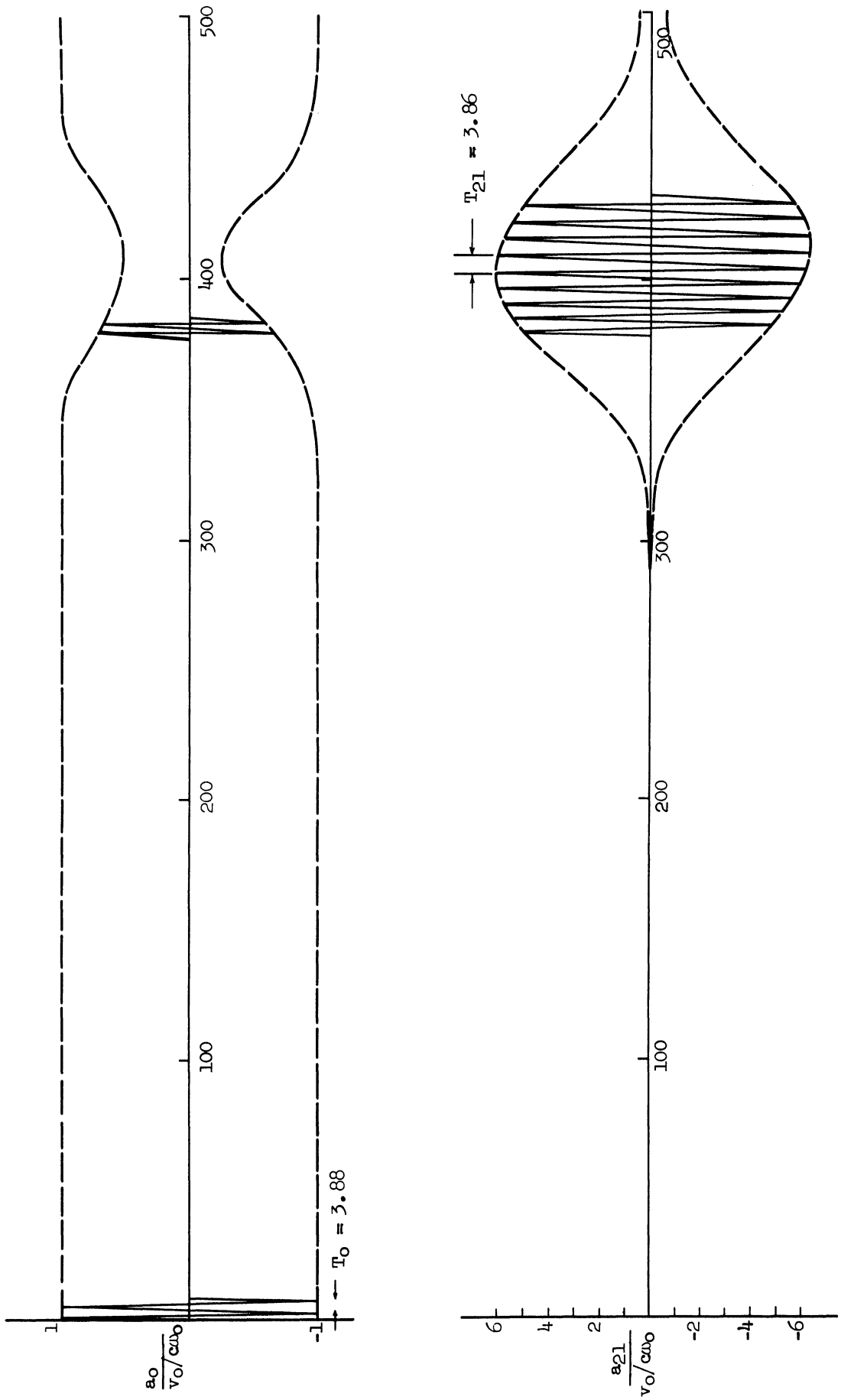

Figure 9. Long-term Behavior for .6 V_{max} .
$a/h = 100$, $\epsilon_n = .05/n^3$

APPENDIX

In Section 3.3 an impulsive pressure acting on a spherical shell is assumed to impart a velocity distribution $\partial w/\partial t$ symmetric about the polar axis. This distribution can be represented as

$$\frac{\partial w}{\partial t} = \sum_{n=0}^{\infty} V_n P_n (\text{Cos } \xi) \tag{A1}$$

The Legendre polynomials of the first kind may be expressed in cosine expansions (see, for example, Magnus and Oberhettinger[14], p. 50). The expansion is

$$P_n(\text{Cos } \xi) = \frac{(2n)!}{2^{2n}(n!)^2}\left[\text{Cos } n\xi + \frac{1}{1}\cdot\frac{n}{2n-1}\text{Cos }(n-2)\xi + \frac{1\cdot 3}{1\cdot 2}\cdot\frac{n(n-1)}{(2n-1)(2n-3)}\text{Cos}(n-4)\xi + \ldots\right] \tag{A2}$$

The brackets contain n+1 terms.

The momentum along the polar axis M_z is

$$M_z = \int_{\text{Area}} \rho h \frac{\partial w}{\partial t}\, d(\text{Area}) \tag{A3}$$

Substitution of (A1) and (A2) into (A3) and integrating yields

$$M_z = -\Pi \rho a^2 \sum_{n \text{ odd}}^{\infty} V_n S_n \tag{A4}$$

where

$$S_n = \frac{(2n)!}{2^{2n}(n!)^2}\left[\frac{4}{4-n^2} + \frac{1}{1}\cdot\frac{n}{2n-1}\cdot\frac{4}{4-(n-2)^2} + \frac{1\cdot 3}{1\cdot 2}\cdot\frac{n(n-1)}{(2n-1)(2n-3)}\cdot\frac{4}{4-(n-4)^2} + \ldots\right]$$

Again the brackets include n+1 terms.

Expression (A4) corresponds to imparting to the center of mass of the shell a velocity $\tilde{V}$ along the polar axis,

$$\tilde{V} = -\frac{1}{4} \sum_{n\ \mathrm{odd}}^{\infty} v_n S_n \tag{A5}$$

The distribution $\partial w/\partial t$ is now considered relative to a shell whose center of mass is moving with velocity $\tilde{V}$. This relative distribution will contribute only to shell deformation. It is

$$\frac{\partial w}{\partial t} = v_\theta + \left[v_1 - \frac{1}{4} \sum_{n\ \mathrm{odd}}^{\infty} v_n S_n\right] P_1(\mathrm{Cos}\ \xi) + \sum_{n=2}^{\infty} v_n P_n(\mathrm{Cos}\ \xi) \tag{A6a}$$

$$\frac{\partial u}{\partial t} = \frac{1}{4} \sum_{n\ \mathrm{odd}}^{\infty} v_n S_n \mathring{P}_1(\mathrm{Cos}\ \xi) \tag{A6b}$$

where $\tilde{w}$ and $\tilde{u}$ are radial and meridional displacements respectively.

BIBLIOGRAPHY

1. Lord Rayleigh. " On the Infinitesimal Bending of Surfaces of Revolution", Proceedings of the London Mathematical Society, XIII (1888),p.4.

2. Love, A.E.H. The Mathematical Theory of Elasticity, Dover Publications, New York, 1944.

3. Love, A.E.H. " The Small Free Vibrations and Deformation of a Thin Elastic Shell", Philosophical Transactions of the Royal Society, 179A (1888), p. 491.

4. Lamb, H. " On the Vibrations of a Spherical Shell", Proceedings of the London Mathematical Society", 14 (1882), p. 50.

5. Silbiger, A. " Free and Forced Vibrations of a Spherical Shell", ONR Report U-106-48, December, 1960.

6. Baker, W.E. " Axisymmetric Modes of Vibration of Thin Spherical Shell", The Journal of the Acoustical Society of America, 33 (1961), p. 1749.

7. Naghdi, P.M. and Kalnins, A. " On Vibrations of Elastic Spherical Shells", Journal of Applied Mechanics, 29 (1962), p. 65.

8. Kalnins, A. " Effect of Bending on Vibrations of Spherical Shells", The Journal of the Acoustical Society of America, 36 (1964), p. 74.

9. Lord Rayleigh. " On Maintained Vibrations", Philosophical Magazine, 15 (1883) Series 5, p. 229.

10. Minorsky, N. Nonlinear Oscillations, D. Van Nostrand Company, Inc., Princeton, 1962.

11. Bolotin, V.V. The Dynamic Stability of Elastic Systems, Holden-Day Inc., San Francisco, 1964.

12. Goodier, J.N. and McIvor, I.K. " The Elastic Cylindrical Shell Under Nearly Uniform Radial Impulse", Journal of Applied Mechanics, 31 (1964), p. 259.

13. Hildebrand, F.B. Methods of Applied Mathematics, Prentice-Hall, Inc., Englewood Cliffs, 1956.

14. Magnus, W. and Oberhettinger, F. Formulas and Theorems for the Functions of Mathematical Physics, Chelsea Publishing Company, New York, 1949.

15. McIvor, I.K. and Sonstegard, D.A. " Discussion of 'Effect of Bending on Vibrations of Spherical Shells' ", The Journal of the Acoustical Society of America, 37 (1965), p. 931.

16. Stoker, J.J. Nonlinear Vibrations, Interscience Publishers, Inc., New York, 1950

17. Lubkin, S. and Stoker, J.J. " Stability of Columns and Strings Under Periodically Varying Forces", Quarterly of Applied Mathematics, 1 (1943), p. 215.